PHYSICAL REVIEW D VOLUME 17, NUMBER 11 1 JUNE 1978

Charmonium: The model

E. Eichten,* K. Gottfried, T. Kinoshita, K. D. Lane,* and T.-M. Yan†
Laboratory of Nuclear Studies, Cornell University, Ithaca, New York 14853
(Received 9 February 1978)

A comprehensive treatment of the charmonium model of the ψ family is presented. The model's basic assumption is a flavor-symmetric instantaneous effective interaction between quark color densities. This interaction describes both quark-antiquark binding and pair creation, and thereby provides a unified approach for energies below and above the threshold for charmed-meson production. If coupling to decay channels is ignored, one obtains the "naive" model wherein the dynamics is completely described by a single charmed-quark pair. A detailed description of this "naive" model is presented for the case where the instantaneous potential is a superposition of a linear and Coulombic term. A far more realistic picture is attained by incorporating those terms in the interaction that couple charmed quarks to light quarks. The coupled-channel formalism needed for this purpose is fully described. Formulas are given for the inclusive e^+e^- cross section and for e^+e^- annihilation into specific charmed-meson pairs. The influence of closed decay channels on ψ states below charm threshold is investigated, with particular attention to leptonic and radiative widths.

I. INTRODUCTION

Since the discovery of the J/ψ resonance[1] much theoretical effort has been directed toward understanding the spectrum and decay properties of the J/ψ family.[2,3] The charmonium model[4-7] has emerged as the most successful theory thus far. It interpreted J/ψ (which we abbreviate as ψ) and ψ' as charmed-quark-antiquark ($c\bar{c}$) bound states, and predicted most of the phenomena that were subsequently observed. The discovery[8] of charmed mesons gives strong support to this interpretation. Except for a small number of unresolved (and possibly important) issues, the model also provides a semiquantitative description of the vast body of new data accumulated in e^+e^- colliding-beam experiments in the 3–5-GeV energy range.[3,9] This is the first of two articles that provide a detailed report of our investigation of the charmonium model. (The principal results have been briefly reported in a number of previous publications.[6,10-14]) It is devoted to an exposition of the model and of the associated theoretical framework. The second article will give a systematic comparison with the data.

Our work is based on two underlying assumptions: First, the basic interaction between quarks is assumed to have a color-SU(3) gauge symmetry. In addition to being in the fundamental representation with respect to color, the quarks carry global quantum numbers such as isospin, strangeness, and charm, generically called "flavor". The global SU(4) symmetry of flavor is broken only by quark masses. Thus the strong interactions are flavor independent except for dynamical effects induced by mass differences. It has been widely conjectured[15] that an unbroken color gauge interaction leads to forces that are so strong at large distances that quarks are permanently confined in color-neutral bound states—the mesons and baryons. We also adopt this assumption.

Secondly, the large masses of the ψ resonances and charmed mesons lead to the assumption that the charmed quarks are so heavy that they may be treated nonrelativistically.[4] No one has yet succeeded in calculating the effective form of the interquark forces from quantum chromodynamics,[16] even in the nonrelativistic limit. To fill this gap we postulate that in this limit many of the gross features of the potential between the charmed quarks can be simulated by the potential

$$V(r) = -\frac{\kappa}{r} + \frac{r}{a^2}\,. \tag{1.1}$$

This is chosen to give a simple interpolation between the known Coulomb-type force at short distance and a linear growth of the static potential suggested by some models of quark confinement.[17]

The recent discovery[18] of the $\mu^+\mu^-$ enhancement Υ probably implies the existence of another $Q\bar{Q}$ family,[14] where Q is a quark carrying a new flavor and having a mass of 4–5 GeV. The variation of the spectrum with quark mass m_Q is very sensitive to the form of $V(r)$, and present indications are[19-21] that our ansatz (1.1) may not pass this test. Several other potentials[20,22] have now been proposed that appear to account better for both the ψ and Υ families. On the other hand, these newer models lead to values of $(v/c)^2$ in the ψ family that are uncomfortably large, and if one confines one's attention to the ψ family, as we do here, there is little, if anything, to be gained by abandoning our ansatz (1.1). The detailed calculations

that we shall report, and which were completed before the discovery of Υ, are therefore based on the linear + Coulomb model of $V(r)$.

In order to describe resonances above the threshold for Zweig-allowed decay, and to give an adequate description of e^+e^- collision in the charm threshold region, it is necessary to extend the simple potential model: The possibility of creation of a light-quark pair must be incorporated. We accomplish this by replacing (1.1), or its operator extension,

$$H_I = \frac{1}{2}\int d^3x\, d^3y\, \psi_c^\dagger(\vec{x})\psi_c(\vec{x})\, V(\vec{x}-\vec{y})\, \psi_c^\dagger(\vec{y})\psi_c(\vec{y})\,, \tag{1.2}$$

by[10,23]

$$H_I = \frac{1}{2}\int d^3x\, d^3y : \rho_a(\vec{x})\, \tfrac{3}{4} V(\vec{x}-\vec{y})\rho_a(\vec{y}) :\,, \tag{1.3}$$

where

$$\rho_a(\vec{x}) = \sum_{\text{flavors}} \psi^\dagger(\vec{x})\, \tfrac{1}{2}\lambda_a\, \psi(\vec{x})$$

is the quark contribution to the color-charge-density operator, and $\psi(\vec{x})$ is the quark field operator. This interaction can create quark-antiquark pairs, and also contains the naive potential terms. It has the advantage of being universal, and of allowing pair creation without additional parameters (except for the light-quark mass).

In Sec. II we review the naive charmonium model in which all degrees of freedom but that of the $c\bar{c}$ pair are ignored. We discuss the qualitative aspects of this system: mass spectrum, radiative transition rates, and leptonic decay rates. Detailed information on the eigenvalues, eigenfunctions, and radiative matrix elements of the naive model is given in Appendix A. In Appendix B a sum rule is derived for the electric dipole moments which applies only to purely linear potentials.

Section III is devoted to a discussion of the effects of coupling of hadronic decay channels to the $c\bar{c}$ bound states. The method of including these contributions through the generalized interaction Hamiltonian (1.3) is discussed in detail along with the approximation scheme used in our calculations. A qualitative discussion of the form of the decay amplitudes and the structure of the $c\bar{c}$ Green's functions is presented. Formulas for exclusive channels in e^+e^- annihilation are derived, as well as for the total cross section for $e^+e^- \to$ hadrons. The coupling of the discrete $c\bar{c}$ sector to the charmed-meson continuum also leads to modification of the ψ-family bound states, and thereby to changes of their leptonic widths and $E1$ rates.

A series of appendices (C–F) give detailed derivations and formulas for exclusive and inclusive cross sections, decay amplitudes, and $E1$ rates.

As previously mentioned, the comparison of the model with the data will appear in the second paper of this series.

II. THE $c\bar{c}$ SECTOR IN THE ABSENCE OF DECAY

This section is devoted to what we shall call the naive charmonium model,[6] in which all degrees of freedom but that of the $c\bar{c}$ pair are ignored. This simplification is suggested by the qualitative success of the naive quark model in the old hadronic spectroscopy. However, unlike the $q\bar{q}$ system (henceforth we use q as a generic symbol for the "old" quarks u, d, and s), the nonrelativistic relation between constituent and composite masses prevails for those $c\bar{c}$ states with which we are concerned in this article. This gives a justification for the nonrelativistic treatment of the c quarks in the charmonium model. Another, and related, contrast between the old and new spectroscopies is that a number of low-lying radial excitations are very apparent in the $c\bar{c}$ system, whereas such excitations are almost submerged by the complex continuum in the $q\bar{q}$ systems.

A. The effective Hamiltonian

Although the present knowledge of non-Abelian gauge theory does not provide us with an explicit $c\bar{c}$ interaction, two things appear to be clear: The interaction must provide for confinement, and at short $c\bar{c}$ separations it must conform with the dictates of asymptotic freedom.

These qualitative features of the interaction already permit an educated guess as to the low-lying level structure of charmonium (see Fig. 1). On the other hand, an explicit form for the interaction allows one to compute many detailed properties of the system (e.g., radiative and leptonic widths) that can only be estimated from qualitative considerations. We therefore translate the intuitive picture into an explicit and simple local potential $V(r)$ that contains the two ingredients already mentioned, viz.

$$V(r) = -\frac{\kappa}{r} + \frac{r}{a^2}\,. \tag{2.1}$$

The $1/r$ behavior of the first term is in accordance with asymptotic freedom. However, the strength κ will be treated as a purely phenomenological parameter[24] for reasons discussed later in this subsection. The linear confinement potential r/a^2 is inferred from lattice gauge the-

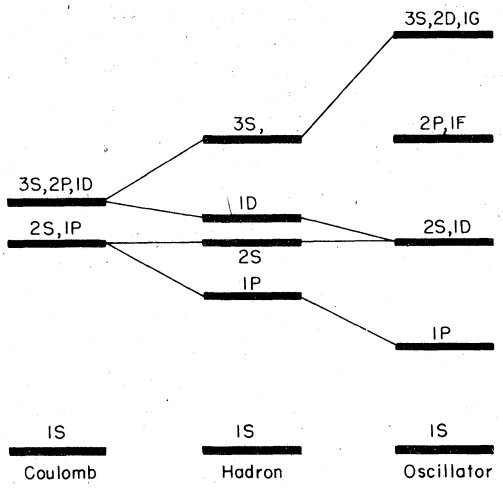

FIG. 1. The qualitative features of the quark-antiquark excitation spectrum can be inferred by visual interpolation, as shown in this figure. Imagine a continuous deformation of an oscillator potential into a Coulomb field, and the associated change of the bound states. The potential of interest in mesonic spectroscopy is between the two extremes, whence the spectrum labeled "hadron". The parameters of the potentials are chosen so that the $2S$-$1S$ difference is fixed. In the case of the "hadron", not all levels are shown for the sake of clarity. Note that we label states by $(n-1)$, where n is the number of radial nodes.

ory[17] and its relation to the dual string model. These considerations indicate that the energy of a widely separated and stationary quark-antiquark pair is proportional to the separation, and that the constant of proportionality $1/a^2$ does not depend on the quark flavor.

Unfortunately these hints from "fundamental" theory only tell us the behavior of V as $r \to 0$ and $r \to \infty$; virtually nothing is known about the intermediate distances. Furthermore, one must suppose that $V(r)$ is the nonrelativistic limit of a far more complex relativistic interaction.[16] This "true" interaction is surely nonlocal on a length scale of order $1/m_c$ which, as we shall see, is small compared with the $c\bar{c}$ states themselves. It must also be spin-dependent, and this will generate something similar to the Breit-Fermi Hamiltonian[21,25] in addition to $V(r)$. We shall have more to say on this score when we compare to the data in the second paper of this series.

In fact, there are experimental indications for the existence of large spin-dependent forces. For instance, if the state observed at 2.83 GeV is in fact $1\,^1S_0$, a very substantial hyperfine interaction must be present in the $c\bar{c}$ system, and it must be repulsive for ^3S states. Such a force might be expected to modify the short-distance behavior of the potential substantially. Another modification of short-distance behavior arises from the asymptotic freedom corrections which produce a logarithmic variation with r of the strength of the Coulomb potential.[16,22]

In order to partially accommodate these short-distance effects within our model we have allowed κ to be a free parameter dissociated from the effective coupling constant α_s determined by the hadronic width of ψ. Instead, the value of κ is determined from the observed data for spin-triplet states, and therefore automatically includes some of the spin-spin contribution.

While our naive ansatz (2.1) for $V(r)$ has the virtue of being unambiguous, and of introducing only a minimum number of parameters, the above discussion, and our earlier remarks about the Υ spectrum, should make its phenomenological nature abundantly clear.

B. Qualitative aspects of the system

Before becoming enmeshed in details, we sketch those qualitative properties that follow from the assumed interaction.

Once the nonrelativistic nature of the system is accepted, it follows that the leptonic width of any $c\bar{c}$ S state with wave function $\psi_n(\vec{r})$ is given by the Van Royen–Weisskopf formula

$$\Gamma(\psi_n \to l\bar{l}) = \frac{16\pi e_c^2 \alpha^2}{M_n^2} |\psi_n(0)|^2, \tag{2.2}$$

where $e_c = \frac{2}{3}$ is the charge of c, and M_n the mass of the state. Assigning $J/\psi(3095) \equiv \psi$ and $\psi(3684) \equiv \psi'$ to $1\,^3S$ and $2\,^3S$, respectively, gives as the observed value

$$r_{21} \equiv \left| \frac{\psi_2(0)}{\psi_1(0)} \right|^2 = 0.62 \pm 0.16 . \tag{2.3}$$

For a pure Coulomb potential $r_{21} = \frac{1}{8}$, while for a purely linear potential $r_{21} \equiv 1$ because all S states have the same $\psi_n(0)$. The value (2.3) shows clearly that the Coulombic potential must be of secondary importance throughout most of the volume over which these states extend.

The constant α_s determines the hadronic $c\bar{c}$ annihilation amplitude, and hence the Zweig-forbidden decay rate of states below charm threshold. For ^3S states this width is

$$\Gamma(\psi_n \to \text{had}) = \frac{160}{81}(\pi^2 - 9)\alpha_s^3 \frac{1}{M_n^2} |\psi_n(0)|^2, \tag{2.4}$$

or

$$\frac{\Gamma(\psi_n \to \bar{l}l)}{\Gamma(\psi_n \to \text{had})} = \frac{6.93 \times 10^{-4}}{\alpha_s^3} . \tag{2.5}$$

For ψ this yields

$$\alpha_s(\psi) = 0.19 \pm 0.03 . \tag{2.6}$$

While α_s is not directly related to the parameter κ in V, the smallness of α_s is consistent with our previous conclusion that the confining interaction is dominant.

If one takes advantage of this, and ignores the Coulombic term altogether, one finds simple scaling laws for all quantities of interest. These serve as useful rules of thumb, and are actually quite reliable for those features that do not depend critically on the wave function near $r = 0$ (e.g., γ-decay matrix elements, states of nonzero angular momentum). Quantities that are sensitive to the $r \approx 0$ region are, however, visibly affected by the Coulombic interaction. The most important examples of the latter type are the leptonic width, and the spin-orbit and spin-spin splittings.

When the Coulomb interaction is ignored, the radial Schrödinger equation can be written as

$$\left(\frac{d^2}{d\rho^2} - \frac{l(l+1)}{\rho^2} - \rho + \zeta\right) u = 0 . \tag{2.7}$$

The dimensionless length ρ and eigenvalue ζ are related to r and the energy E as follows:

$$r = a(m_c a)^{-1/3} \rho , \tag{2.8}$$

$$E = m_c (m_c a)^{-4/3} \zeta . \tag{2.9}$$

Here (and throughout) the u's are normalized by

$$\int_0^\infty u^2(\rho)\, d\rho = 1 ; \tag{2.10}$$

their relation to the conventional radial wave function is

$$R(r) = \left(\frac{m_c}{a^2}\right)^{1/2} \frac{u(\rho)}{\rho} . \tag{2.11}$$

When referring to a particular state, we use the subscript nl (e.g., ζ_{nl}), where $(n-1)$ is the number of radial nodes.

The parameters a and m_c can be determined from the $\psi' - \psi$ mass difference and the leptonic width of ψ. According to (2.9)

$$m_{\psi'} - m_\psi = m_c (a m_c)^{-4/3} (\zeta_{20} - \zeta_{10}) , \tag{2.12}$$

where $\zeta_{20} = 4.088$ and $\zeta_{10} = 2.338$. For a linear potential

$$\lim_{\rho \to 0} \frac{u_{n0}(\rho)}{\rho} = 1 , \tag{2.13}$$

and from (2.2) we thus have

$$\Gamma(\psi \to l\bar{l}) = \tfrac{16}{9} \alpha^2 m_c (a m_\psi)^{-2} . \tag{2.14}$$

Comparison of Eqs. (2.12) and (2.14) with the data yields

$$\begin{aligned} a &= 1.95 \text{ GeV}^{-1} , \\ m_c &= 1.85 \text{ GeV} . \end{aligned} \tag{2.15}$$

The fact that $2m_c = 3.70$ GeV is so close to the charm threshold $W_c = 3.73$ GeV indicates that this is indeed a nonrelativistic system. An independent check of this property is desirable, however, for when $\lim_{r \to \infty} V(r) \neq 0$, the absolute energy scale need not have significance. A reliable characterization is provided by the mean-square velocity,

$$\langle v^2 \rangle = (a m_c)^{-4/3} \int_0^\infty (du/d\rho)^2 \, d\rho . \tag{2.16}$$

For ψ and ψ' this gives $\langle v^2 \rangle = 0.14$ and 0.25, respectively.

These calculations confirm that the gross structure of the system is determined by the confining potential, and that the motion is nonrelativistic to a decent approximation. The qualifications in this last sentence should not be forgotten, however. In determining the parameters a and m_c we used the leptonic width of ψ, and as this quantity depends on the $r \simeq 0$ regime, it is sensitive to short-distance departures from the linear potential. The following analysis, which restores the Coulombic potential, therefore leads to a value of m_c that differs noticeably from the one in (2.15), and to a somewhat larger mean-square velocity.

Accepting the hypothesis that a is a universal constant, and ignoring all relativistic and Coulombic effects, we see from (2.9) that an increase of quark mass m_Q compresses the spectrum by the factor $m_Q^{-1/3}$. The size of the system, and therefore all $E1$ matrix elements, also scale by the factor $m_Q^{-1/3}$.

C. Inclusion of the Coulombic interaction

The Coulombic interaction adds the term λ/ρ to the Schrödinger equation (2.7), where

$$\lambda = \kappa (m_c a)^{2/3} . \tag{2.17}$$

We continue to denote eigenvalues and eigenfunctions by ζ_{nl} and u_{nl}, but these are now functions of λ. The dependence of the spectrum on λ is shown in Fig. 2, and given in greater detail in Appendix A. Note that the ordering of levels in Fig. 2 agrees with the intuitive argument summarized by Fig. 1. Graphical and numerical information concerning the eigenfunctions and eigenvalues can also be found in Appendix A.

Inclusion of the Coulombic term does not alter the relation (2.12) between a, m_c, and the $\psi - \psi'$ mass difference, except for the implict dependence of the eigenvalues on λ. The formula (2.14) for $\Gamma(\psi_n \to l\bar{l})$ does change, however, because

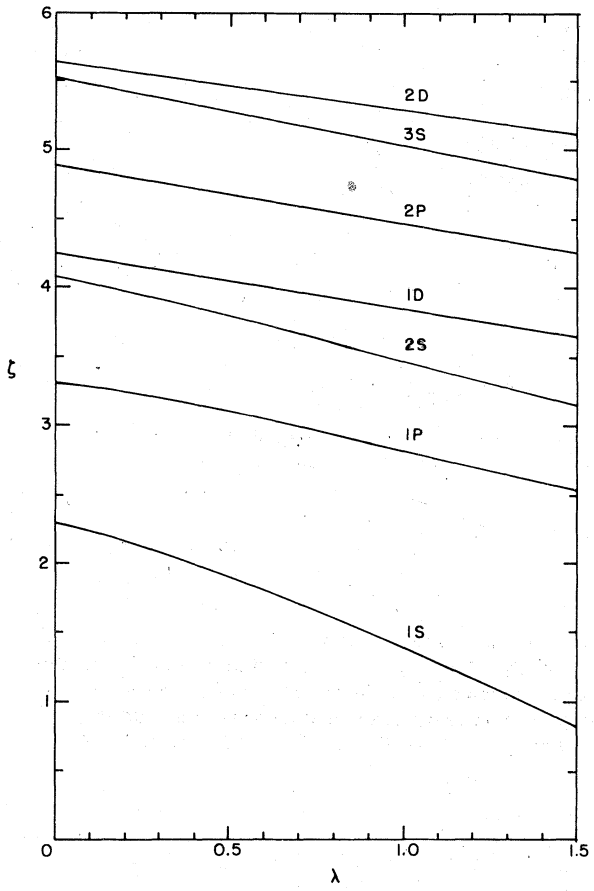

FIG. 2. Energy eigenvalues for the Coulomb+linear potential. The dimensionless eigenvalue ζ is related to the energy by $E=m_c(m_c a)^{-4/3}\zeta$ [cf. Eq. (2.9)], and the strength of the Coulombic potential is given by $\kappa=\lambda(m_c a)^{-2/3}$ [cf. Eq. (2.17)]; when $\lambda=0$, the potential is purely linear. Observe that the level ordering agrees with Fig. 1.

(2.13) is no longer valid. Instead, one has the theorem that for any S state,[6,26]

$$|\psi_{n0}(0)|^2=\frac{m_c}{4\pi}\int|\psi_{n0}(r)|^2\frac{\partial V}{\partial r}\,d^3r\,. \tag{2.18}$$

In our case this reduces to

$$|\psi_{n0}(0)|^2=\frac{m_c}{4\pi a^2}(1+\lambda\langle\rho^{-2}\rangle_{n0})\,, \tag{2.19}$$

where

$$\langle f\rangle\equiv\int_0^\infty[u(\rho)]^2 f(\rho)d\rho\,. \tag{2.20}$$

A tabulation of $\langle\rho^{-2}\rangle$ can be found in Appendix A.

D. Radiative transitions

The $E1$ transition rate is given by

$$\Gamma_{E1}=\tfrac{4}{27}\,e_c^{\,2}\,\alpha\,\frac{a^2}{(m_c a)^{2/3}}\,k^3\,|E_{if}|^2(2J_f+1)S_{if}\,, \tag{2.21}$$

where k is the photon momentum, S_{if} is a statistical factor, and

$$E_{if}=\int_0^\infty u_i(\rho)u_f(\rho)\rho\,d\rho \tag{2.22}$$

is the dipole matrix element. As one would expect, E_{if} is quite insensitive to the Coulombic interaction, because (2.22) favors large values of ρ. (A detailed tabulation of E_{if} is given in Appendix A.) Since level spacings vary approximately as $m_c^{-1/3}$, we see that $E1$ rates for "heavy quark" systems are related to charmonium by

$$\Gamma_{E1}(Q\bar{Q})\simeq\left(\frac{e_Q}{e_c}\right)^2\left(\frac{m_c}{m_Q}\right)^{5/3}\Gamma_{E1}(c\bar{c})\,. \tag{2.23}$$

Our statistical factor is defined so that $S_{if}=S_{fi}$. Moreover, $S_{if}=1$ for all $^3S\to{}^3P$ transitions, and $S_{if}=3$ for any $E1$ transition between spin singlets. A table of values for S_{if} can be found in Ref. 14.

The $M1$ transition rate between ^3S and ^1S states is

$$\Gamma_{M1}=\left(\frac{e_c}{2m_c}\right)^2\alpha k^3|M_{if}|^2(2J_f+1)\,, \tag{2.24}$$

where we assume a Dirac moment for the quark, and

$$M_{if}=\int_0^\infty u_i(\rho)u_f(\rho)j_0[ka(m_c a)^{-1/3}\rho/2]\,d\rho\,. \tag{2.25}$$

For transitions between hyperfine partners, $M_{if}\simeq 1$, but for transitions between different multiplets (e.g., $\psi'\to\eta_c\gamma$), M_{if} is very small because u_f and u_i are orthogonal, and $j_0\simeq 1$. A graph of M_{if} for the transitions of interest is provided in Fig. 12 of Appendix A.

III. COUPLING BETWEEN THE $c\bar{c}$ AND DECAY SECTORS

The model described in Sec. II has a serious shortcoming common to virtually all models of the hadron spectrum: It ignores the fact that hadronic states are, with but rare exceptions, highly unstable. We now address ourselves to removing this shortcoming.

A. Qualitative features of decay amplitudes

The Zweig rule provides a remarkably significant (and ill understood) classification of hadronic decay modes. Zweig-forbidden decays have par-

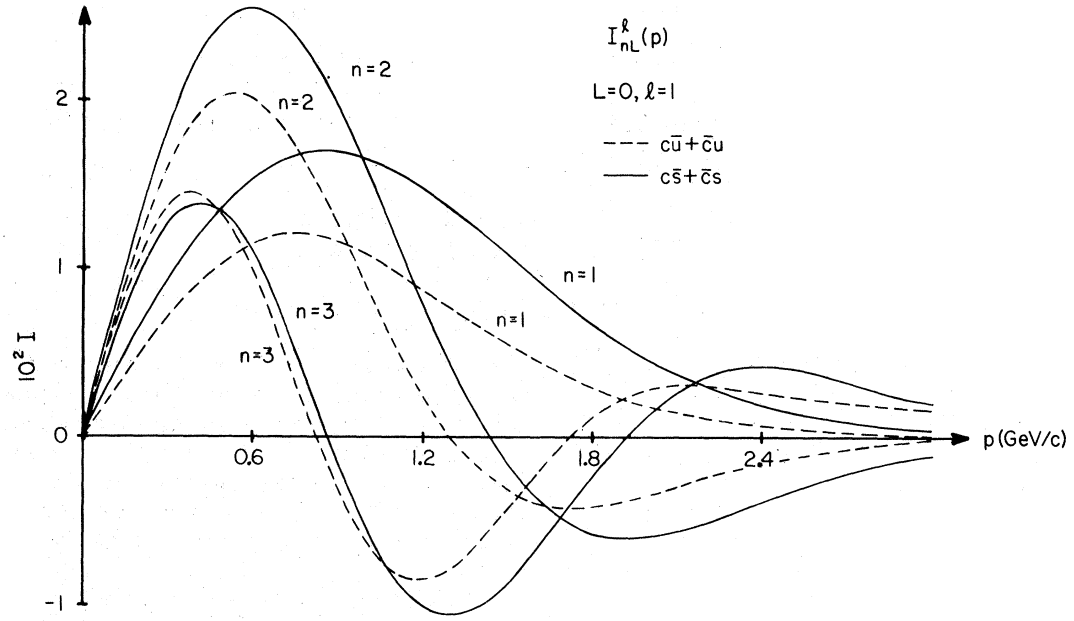

FIG. 3. P-wave decay amplitudes for $c\bar{c}\,^3S$ states. The quantity plotted is $I^l_{nL}(p)$, defined in Eq. (3.37) where n and L are the principal quantum number and orbital angular momentum of the $c\bar{c}$ state, and l the orbital angular momentum of the decay products whose relative momentum is p. The dashed line applies to the decays $c\bar{c}\to c\bar{u}+\bar{c}u$ (or $c\bar{d}+\bar{c}d$), the solid line to $c\bar{c}\to c\bar{s}+\bar{c}s$; the former is therefore used for decays to nonstrange charmed mesons (e.g., $D^*\bar{D}^*$), the latter for decays involving F and/or F^*. The quark masses are $m_{u,d}=0.33$ GeV, $m_s=0.50$ GeV, and $m_c=1.65$ GeV, while $a=2.07$ GeV^{-1}.

tial widths that are much smaller than level spacings, and can be incorporated as an afterthought, i.e., in perturbation theory. Zweig-allowed decay widths are too broad to be handled perturbatively. Amongst effects that fall outside the scope of perturbation theory of particular importance in the charmonium system are strongly momentum-dependent decay amplitudes that can lead to rapid variations of branching fractions and highly distorted resonances, additional resonance distortion due to the proximity of thresholds, and mixing between levels of the primordial discrete spectrum due to their coupling to common decay channels.

Since hadrons are extended systems, one must expect their decay amplitudes to have a momentum dependence that is more intricate than that given by the angular momentum barrier. Whatever may be the detailed dynamical mechanism responsible for decay, the amplitude for a two-body decay involves an overlap integral between three extended wave functions. Beyond the angular momentum factors these wave functions are usually approximated by a monotonically decreasing form factor. This is adequate insofar as one does not deal with radially excited states. Once such excitations come into play, however, the overlap integrals must be expected to have nodes. This is illustrated in Figs. 3 and 4 which show the decay amplitudes for

$$n\,^3S_1(c\bar{c})\to C_1\bar{C}_2 \quad \text{and} \quad n\,^3D_1(c\bar{c})\to C_1\bar{C}_2, \tag{3.1}$$

where C_α is a charmed 0^- or 1^- meson. (We will associate $3\,^3S$ and $4\,^3S$ states with the structures in $e^+e^-\to$ hadrons observed at 4.028 and 4.414 GeV.) Clearly there is a strong correlation between the number of radial nodes in the parent state and the number of nodes in the decay amplitude.[11] The precise position of these nodes depends on the assumed decay mechanism. But the general features shown in these figures are presumably more than an artifact of our model.

There is another reason for uncommonly rapid variations of decay amplitudes for the reactions $c\bar{c}\to c\bar{q}+\bar{c}q$. A fermion-antifermion bound state occupies a volume that is inversely proportional to the reduced mass. Thus the $c\bar{c}$ system is considerably smaller than its decay products, in contrast to the "old" spectroscopy where parents and daughters are of the same size.

The nodal structure of these decay amplitudes can yield a dramatic energy dependence of exclusive cross sections; for example, $\sigma(e^+e^-\to D\bar{D})$ goes through a zero in the neighborhood of 4 GeV, and therefore accounts at least qualitatively for the astonishing branching fractions[27]

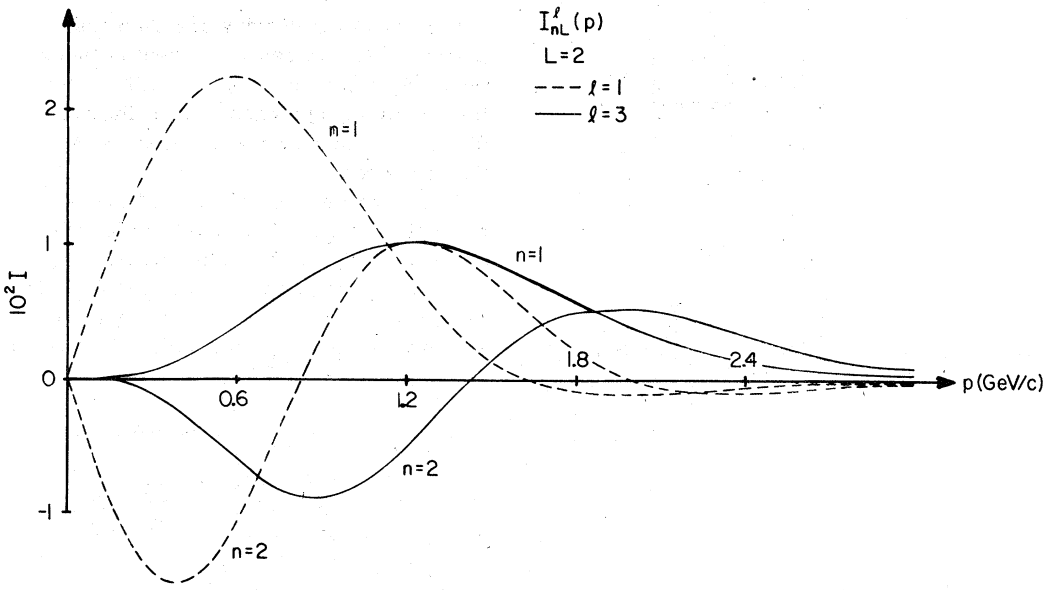

FIG. 4. P- and F-wave nonstrange decay amplitudes for $c\bar{c}$ $^3D_1$ states. Parameters are as in Fig. 3.

$D\bar{D}/D^*\bar{D}^*$ in that region.[13,21,28] We shall discuss this matter in some detail in the second paper of this series.

As Eq. (3.1) and Figs. 3 and 4 demonstrate, a given decay channel $C_1\bar{C}_2$ can communicate with both $^3S_1$ and $^3D_1$ $c\bar{c}$ states, and therefore mixes them. It is this effective tensor force[10,13] that accounts for the leptonic width[29] of $\psi(3772)$.

B. The decay mechanism

The decay mechanism must describe how the spatial separation of the $c\bar{c}$ pair leads to the creation of a light $q\bar{q}$ pair. Here again color gauge theory provides only an intuitive framework, not an explicit formula. Indeed, the correct form of the decay amplitude might be very complicated—too complicated, in fact, for the rather complex calculations that follow. Once more we must resort to improvization, and as before, our guiding principle is simplicity. Specifically, we assume that the instantaneous interaction which causes the binding of $c\bar{c}$ and $q\bar{q}$ states is *also* responsible for the decay. That is, we assume a four-fermion interaction[30]

$$H_I = \frac{1}{2}\sum_{a=1}^{8}\int :\rho_a(\vec{\mathbf{r}})\,V_0(\vec{\mathbf{r}}-\vec{\mathbf{r}}')\rho_a(\vec{\mathbf{r}}'):d^3r\,d^3r', \tag{3.2}$$

where

$$\rho_a(\vec{\mathbf{r}}) = \psi^\dagger(\vec{\mathbf{r}})\tfrac{1}{2}\lambda_a\psi(\vec{\mathbf{r}}) \tag{3.3}$$

is the octet of color densities of the quark field ψ.

The potential V of Sec. II is related to that in (3.2) by $V=\frac{4}{3}V_0$. In order to simplify our calculations, we ignore the Coulombic part of V_0 (in both wave functions and interaction) in evaluating the decay amplitudes. This is certainly justified because we already saw that the confining potential dominates; furthermore, small quark separations are not important in hadronic decays. On the other hand, the major effects of the Coulomb term are included by use of the full potential V_0 in the calculation of masses and leptonic widths for $c\bar{c}$ states. Due to the presence of decay channels, however, the value of the parameters a and m_c will differ somewhat from the one used in Sec. II (see Sec. III E).

When ψ is decomposed into destruction and creation operators, (3.2) generates a large number of terms (see Fig. 5). There is an attractive interaction $\frac{4}{3}V_0$ between $c\bar{c}$ pairs, and if everything else were ignored, this would give the "naive" charmonium model of Sec. II. There is also the $q\bar{q}$ attraction that produces the "old" mesons, and a $c\bar{q}$ attraction responsible for charmed mesons. But there are also terms where, for example, a $c\bar{c}$ pair creates or destroys a $q\bar{q}$ pair. These are the terms that describe decay. By our ansatz (3.2), we have decreed that such decay amplitudes are simply related to the binding potential V_0, and therefore contain no new parameters whatsoever.

It is abundantly clear that our assumption of one instantaneous interaction responsible for both binding and decay is very simplistic. Nevertheless,

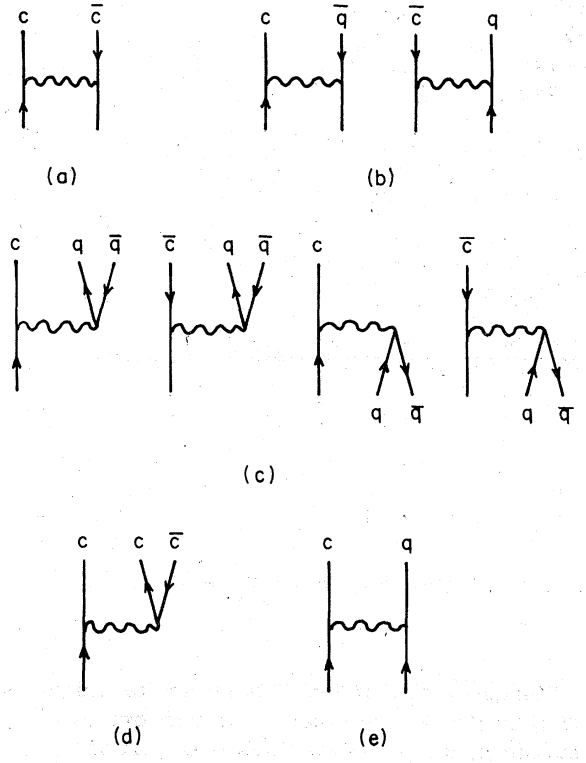

FIG. 5. Terms in the model Hamiltonian, Eq. (3.2). The wavy line is the instantaneous potential V_0. Here (a) shows interactions in the $c\bar{c}$ sector; (b) interactions that bind charmed mesons; (c) interactions that lead to the Okubo-Zweig-Iizuka-rule-allowed decays considered here; (d) interactions that go outside the usual framework of the naive quark model, and ignored by us; and (e) terms that contribute to final-state interactions, and ignored here.

as we shall see, this model has enough structure to produce the rather complicated decay phenomena with which we must deal. Given the complexity of these phenomena and the attendant calculations it is actually an asset to have so tightly constrained a model. Otherwise one is in danger of disappearing in a fog of adjustable parameters.

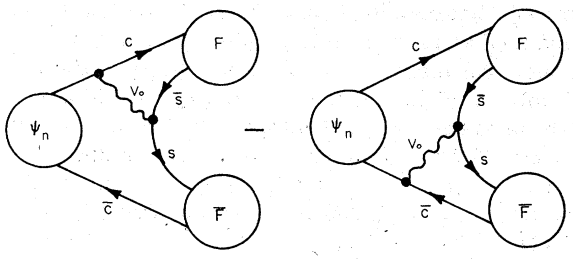

FIG. 6. This diagram depicts the decay of a $c\bar{c}$ state ψ_n into $F\bar{F}$. There are two terms, corresponding to $s\bar{s}$ creation by c or $\bar{c}$. The formula corresponding to this is Eq. (3.33).

The decay amplitudes are then just matrix elements of H_I between the parent $c\bar{c}$ state, and the two-body final-state $c\bar{q}+\bar{c}q$. Their structure can be depicted graphically, as in Fig. 6, which shows $c\bar{c}\to F\bar{F}$. A more detailed discussion of these amplitudes appears in Sec. III F.

What then remains is to evaluate the consequences of the coupling between the discrete $c\bar{c}$ and the continuous $c\bar{q}+\bar{c}q$ sectors. In essence, this is a generalization of the natural line-broadening problem, and the formalism described below[31] is just an elaboration of the Weisskopf-Wigner solution of that problem.

C. The resolvents

It is convenient to decompose the Hilbert space $\mathcal{H}$ into the $c\bar{c}$ sector $\mathcal{H}_\psi$, the decay sector $\mathcal{H}_C$, and a remainder $\mathcal{H}_R$, and introduce the corresponding projection operators P_ψ, P_C, and P_R. The total Hamiltonian, i.e., the interaction H_I of Eq. (3.2) plus the quark kinetic energy, can then be written as

$$H=H_\psi+H_C+U+U^+ +H', \tag{3.4}$$

where

$$H_\psi=P_\psi HP_\psi\,,\quad H_C=P_C HP_C \tag{3.5}$$

and U is the operator whose matrix elements are the decay amplitudes discussed previously:

$$U=P_\psi H_I P_C\,. \tag{3.6}$$

H_ψ contains those portions of H_I that bind $c\bar{c}$ pairs into the "naive" charmonium states. H_C contains the $c\bar{q}$ and $\bar{c}q$ interactions that bind charmed mesons, as well as matrix elements of H_I that describe final-state interactions between $c\bar{q}$ and $\bar{c}q$ systems.

Most quantities of interest to us are conveniently expressed in terms of the resolvent $\mathcal{G}(z)$ in the $c\bar{c}$ sector,

$$\mathcal{G}(z)=P_\psi\frac{1}{z-H}P_\psi\,. \tag{3.7}$$

$\mathcal{G}$ provides a complete description of the $c\bar{c}$ sector in the presence of decay channels, whether open or closed. We also need the resolvent in the $c\bar{q}+\bar{c}q$ (or decay) sector

$$\mathfrak{D}(z)=P_C\frac{1}{z-H}P_C\,. \tag{3.8}$$

By locating the poles of $\mathcal{G}$ on the real z axis, we can determine the eigenvalues of $c\bar{c}$ bound states, including their displacement due to the presence of closed decay channels. Let E_n be the position of such a pole. The residue of $\langle\vec{r}|\mathcal{G}(z)|\vec{r}'\rangle$ at $z=E_n$ is proportional to $\Psi_n(\vec{r})\Psi_n^*(\vec{r}')$, where $\Psi_n(\vec{r})$ can be interpreted as the bound-state wave function in

the $c\bar{c}$ sector *including* the effects of decay couplings. (Here $\vec{r}$ is the separation of the $c\bar{c}$ pair. All other variables are suppressed for now; they will be made explicit in Sec. III F.) $\Psi_n(\vec{r})$ can be expanded in terms of the orthonormal eigenfunctions $\psi_k(\vec{r})$ of H_ψ (which describes the uncoupled system) as

$$\Psi_n(\vec{r})=\sum_k a_k^{(n)}\psi_k(\vec{r})\,. \tag{3.9}$$

The expansion coefficients satisfy

$$\sum_k |a_k^{(n)}|^2<1 \tag{3.10}$$

because $\Psi_n(\vec{r})\Psi_n^*(\vec{r})$ is in general not the residue of the full resolvent $\langle\vec{r}|1/(z-H)|\vec{r}'\rangle$. The amplitude for finding the configuration $c\bar{q}+\bar{c}q$ in the bound state n is obtained from the residue of $\mathfrak{D}$ at the same pole. A knowledge of $\Psi_n(\vec{r})$, and of the virtual decay amplitude, is necessary for the calculation of the radiative decays discussed in Sec. III H.

$\mathcal{G}$ and $\mathfrak{D}$ have branch cuts for $\mathrm{Re}z>W_c$, where W_c is the threshold for Zweig-allowed decay, $W_c=2m_D$. (We ignore the very weak cuts due to Zweig-forbidden decays.) The discontinuities across these cuts are directly related to observable quantitites. For example $\mathrm{Disc}\langle\vec{r}|\mathcal{G}(W)|\vec{r}\rangle$ is proportional to the probability of finding a $c\bar{c}$ pair of total energy W at separation $\vec{r}$. When evaluated at $\vec{r}=0$, $\mathrm{Disc}\mathcal{G}$ is thus proportional to the cross section for $e^+e^-\to c\bar{c}\to$ hadrons. The complete expression for the contribution of charm to the ratio R is found to be

$$\Delta R(W)=-\frac{32\pi}{W^2}\lim_{r\to 0}\mathrm{Im}\langle\vec{r}|\mathcal{G}(W+i0)|\vec{r}\rangle\,. \tag{3.11}$$

A detailed derivation of (3.11) is given in Appendix C. In Sec. III G we shall also show how $\Delta R(W)$ can be split into contributions from various exclusive channels.

D. The coupled-channel equations

We now set up approximate equations for $\mathcal{G}$ and $\mathfrak{D}$. The procedure we adopt is a time-honored one that ultimately goes back to Weisskopf and Wigner, and has been applied to such diverse phenomena as nuclear reactions, K^0 decays, and collision broadening.[31,32]

As was outlined in Sec. III C, we first divide the Hilbert space $\mathcal{H}$ into the $c\bar{c}$ sector $\mathcal{H}_\psi$, the decay sector $\mathcal{H}_C$, and a remainder $\mathcal{H}_R$, and decompose the Hamiltonian H as in (3.4) with the help of the P_ψ, P_C, and P_R. Then an equation for $\mathcal{G}$ follows from the identity

$$\frac{1}{z-H}=\frac{1}{z-H_\psi}+\frac{1}{z-H_\psi}(H-H_\psi)\frac{1}{z-H}\,, \tag{3.12}$$

viz.,

$$\mathcal{G}=G+GP_\psi(H-H_\psi)(P_C+P_R)\frac{1}{z-H}P_\psi\,, \tag{3.13}$$

where

$$G(z)=P_\psi\frac{1}{z-H_\psi}P_\psi \tag{3.14}$$

is the resolvent of the "naive" model. The kernel in (3.13) can be rewritten as

$$P_\psi(H-H_\psi)(P_C+P_R)=U+P_\psi H_I P_R\,,$$

where $P_\psi H_I P_R$ contains transitions from the $c\bar{c}$ sector to the $(c\bar{c},\bar{c}c)$ sector. Relying on the many successes of the quark model, we only retain valence quarks, and delete components of state with extra pairs, thereby reducing (3.13) to

$$\mathcal{G}=G+GUP_C\frac{1}{z-H}P_\psi\,. \tag{3.15}$$

An equation for the off-diagonal portion of the resolvent follows from the identity

$$\frac{1}{z-H}=\frac{1}{z-H_C}+\frac{1}{z-H_C}(H-H_C)\frac{1}{z-H}\,,$$

i.e.,

$$P_C\frac{1}{z-H}P_\psi=D(z)P_C H_I(P_\psi+P_R)\frac{1}{z-H}P_\psi\,, \tag{3.16}$$

where

$$D(z)=P_C\frac{1}{z-H_C}P_C$$

is the resolvent in the decay sector in the absence of coupling to other sectors. In (3.16), $P_C H_I P_R$ describes two types of processes: (i) decays that are forbidden by Zweig's rule, such as $c\bar{c}\to s\bar{s}$; (ii) transitions between the two-pair and three-pair sectors, e.g., the Zweig-allowed processes $D\bar{D}\to D\bar{D}^*\pi$ and $D\bar{D}^*\to D\bar{F}K$, or the Zweig-forbidden $F\bar{F}\to F\bar{F}^*\psi$. Continuing with our semiempirical approach, we drop all Zweig-forbidden amplitudes. As for the two-to-three-pair amplitudes, we also drop these because of the observed dominance of quasi-two-body decays. (Note that this does not mean that our final states are restricted to two-hadron states; $\mathcal{H}_C$ contains states such as $D^*\bar{D}^*$, which are observed as the four-body final state $D\bar{D}\pi\pi$.) Having ignored $P_C H_I P_R$ altogether, we can reduce (3.16) to

$$P_C\frac{1}{z-H}P_\psi\simeq DU^\dagger\mathcal{G}\,. \tag{3.17}$$

This closes our system of equations,

$$\mathcal{G}=G+GUDU^\dagger\mathcal{G}\,. \tag{3.18}$$

Similarly, we find

$$\mathfrak{D} = D + DU^{\dagger}GU\mathfrak{D}. \tag{3.19}$$

Equations (3.18) and (3.19) are our basic equations. Virtually all the results reported in the remainder of these papers devolve from them.

E. Solving the coupled-channel equations for $\mathcal{G}$

One can transform (3.18) into a set of linear algebraic equations. For this purpose, introduce the eigenfunctions $\psi_n(\vec{r})$ and eigenvalues ϵ_n of the "naive model"—i.e., of H_ψ. Then

$$\langle \vec{r}' | \mathcal{G}(z) | \vec{r} \rangle = \sum_n \psi_n(\vec{r}') \langle n | \mathcal{G}(z) | \vec{r} \rangle . \tag{3.20}$$

From (3.18)

$$\langle n | \mathcal{G}(z) | \vec{r} \rangle = \langle n | G(z) | \vec{r} \rangle + \frac{1}{z - \epsilon_n} \sum_m \Omega_{nm}(z) \langle m | \mathcal{G}(z) | \vec{r} \rangle , \tag{3.21}$$

where

$$\Omega_{nm}(z) = \langle n | UD(z)U^{\dagger} | m \rangle . \tag{3.22}$$

The matrix Ω is of central importance: it describes the coupling between the primordial $c\bar{c}$ levels due to the presence of open and closed decay channels.

As explained earlier, the states that diagonalize $D(z)$ are the $q\bar{c} + \bar{q}c$ states, i.e., states composed of two mesons with charm 1 and −1. For now we designate such a state by $|\tau \vec{p}_1 \vec{p}_2\rangle$, where τ specifies all discrete quantum numbers such as strangeness, helicity, etc., while $(\vec{p}_1, E_1)$ and $(\vec{p}_2, E_2)$ are the momenta and energies of the two mesons. Then

$$\Omega_{nm}(z) = \sum_\tau \int d^3p_1 \, d^3p_2 \times \frac{\langle n | U | \tau \vec{p}_1 \vec{p}_2 \rangle \langle m | U | \tau \vec{p}_1 \vec{p}_2 \rangle^*}{z - E_1 - E_2} . \tag{3.23}$$

Strictly speaking, the states $|\tau \vec{p}_1 \vec{p}_2\rangle$ should include final-state interactions, because $P_C H_I P_C$ does contain such terms. However, final-state interactions of finite range do not have dramatic consequences. All they ever do is to produce slow modulations of various quantities. For example, they provide a slowly varying phase shift in $D\bar{D} \to D\bar{D}$ elastic scattering in addition to the rapid variation due to the resonant process $D\bar{D} \to c\bar{c} \to D\bar{D}$. As we are mainly concerned with resonances, and rapid energy variations in general, we shall henceforth ignore final-state interactions.

Returning to (3.21), we note that the free resolvent G is

$$G(z) = \sum_n \frac{|n\rangle\langle n|}{z - \epsilon_n} ,$$

and therefore

$$\langle n | G(z) | \vec{r} \rangle = \frac{\psi_n^*(\vec{r})}{z - \epsilon_n} .$$

Hence

$$\langle n | \mathcal{G}(z) | \vec{r} \rangle = \frac{1}{z - \epsilon_n} \left[\psi_n^*(\vec{r}) + \sum_m \Omega_{nm}(z) \langle m | \mathcal{G}(z) | \vec{r} \rangle \right] . \tag{3.24}$$

This is the promised set of linear equations.

Once (3.24) is solved, the complete resolvent can be constructed from (3.20). In particular, the inclusive ratio $\Delta R(W)$, as given by (3.11), is

$$\Delta R(W) = -\frac{32\pi}{W^2} \lim_{r \to 0} \operatorname{Im} \sum_n \psi_n(0) \langle n | \mathcal{G}(W + i0) | \vec{r} \rangle . \tag{3.25}$$

To illustrate the content of these equations, we briefly consider the *unjustified* approximation $\Omega_{nm}(z) = \delta_{nm}\omega_n(z)$. Solving (3.24) with this ansatz, we immediately find

$$\langle \vec{r} | \mathcal{G}(z) | \vec{r}' \rangle = \sum_n \frac{\psi_n(\vec{r}) \psi_n^*(\vec{r}')}{z - \epsilon_n - \omega_n(z)} . \tag{3.26}$$

In this simple example, the eigenfunctions are unaffected by the coupling except for an overall factor to account for leakage to the decay sector. The ratio ΔR is thus

$$\Delta R(W) = \frac{32\pi}{W^2} \sum_n \frac{|\psi_n(0)|^2 \operatorname{Im}\omega_n(W + i0)}{|W - \epsilon_n - \omega_n(W + i0)|^2} , \tag{3.27}$$

which is a variant of the generalized vector-meson-dominance model.[33] Note that even in this simple case, we are by no means restricted to an energy independent width. Indeed, if there are nearby thresholds, or rapidly varying decay amplitudes in ω_n, (3.27) can lead to shapes that are very far from a superposition of simple Lorentzians.

In our actual calculations we truncate the set of linear equations (3.24) by replacing $\mathcal{H}_\psi$ by a finite-dimensional vector space spanned by the lowest N states $\{|n\rangle\}$ having a definite angular momentum and parity. This approximation makes sense for low-lying states because the decay amplitudes $\langle n | U | \tau \vec{p}_1 \vec{p}_2 \rangle$ fall off very rapidly as $|E_1 + E_2 - \epsilon_n| \to \infty$. As a consequence the coupling matrix Ω_{nm} decreases rapidly as one moves off the diagonal, and the accuracy of the calculation can be controlled by increasing N. For example, we find that $N \simeq 6$ is adequate for low $^3S_1$ and $^3D_1$ states.

Once the matrix Ω is known, the eigenvalues of the coupled system are found from

$$\operatorname{Det} | (z - \epsilon_n)\delta_{nm} - \Omega_{nm}(z) | = 0 . \tag{3.28}$$

For $\operatorname{Re} z < W_c$, where $W_c = 2m_D$ is the charm threshold, these zeros lie on the real axis and locate

the bound-state energies. The parameters of the model are determined, as before, from $|m_{\psi'} - m_\psi|$ and the leptonic width of ψ. Because of the level shifts and modifications of wave functions, these "renormalized" parameters differ somewhat from those of the "naive" model of Sec. II. The details of this procedure will be discussed in the second paper of this series.

F. The decay amplitudes and the matrix Ω_{nm}

In order to compute the decay amplitude $\langle n|U|\tau\vec{p}_1\vec{p}_2\rangle$ we must first construct the state vectors for the decay products. In constructing these states, and also in evaluating the decay amplitude itself, we shall make an important approximation: All expressions will be reduced to their nonrelativistic limits. As we have seen, this approximation is reasonable in the $c\bar{c}$ sector, but it is not really applicable to the decay sector which contains light quarks. The only justification is simplicity; a relativistic treatment is necessarily much more complex, and there is actually no established relativistic treatment of bound states for a confining interaction. Furthermore, there is no reason to believe that a relativistic theory would introduce new qualitative features that are not already present in our nonrelativistic treatment.

Let C_α be a charmed meson of type α, momentum $\vec{P}$, and helicity λ. Then, its wave function ϕ_α is defined by

$$|C_\alpha(\vec{P}\lambda)\rangle = \frac{1}{\sqrt{3}} \sum_{as_1s_2} \int d^3p_1\, d^3p_2\, \delta^3(\vec{P} - \vec{p}_1 - \vec{p}_2) \times \phi_\alpha(\vec{P}\lambda; \vec{p}_1 s_1 \vec{p}_2 s_2) b^\dagger_{ca}(\vec{p}_1 s_1) \times d^\dagger_{qa}(\vec{p}_2 s_2)|0\rangle , \quad (3.29)$$

where $b^\dagger_{ca}$ creates a charmed quark of color a and the indicated momentum and spin projection, while $d^\dagger_{qa}$ creates $\bar{q}$. This is to be an eigenfunction of H_C,

$$[H_C - (P^2 + M_\alpha^2)^{1/2}]|C_\alpha(\vec{P}\lambda)\rangle = 0 .$$

The nonrelativistic eigenvalue ϵ_α is defined by

$$(P^2 + M_\alpha^2)^{1/2} \to M + (P^2/2M) + \epsilon_\alpha ,$$

where $M = m_c + m_q$. The Schrödinger equation for ϕ is

$$\left(\frac{p^2}{2\mu} - \epsilon_\alpha\right) \phi_{\alpha\lambda}(\vec{p}s_1s_2) = \tfrac{4}{3} \int d^3p' \int \frac{d^3r}{(2\pi)^3} e^{i(\vec{p}-\vec{p}')\cdot\vec{r}} \times V_0(\vec{r})\phi_{\alpha\lambda}(\vec{p}'s_1s_2) , \quad (3.30)$$

where $\vec{p}$ is the relative momentum and μ the reduced mass of the $c\bar{q}$ system. In the nonrelativistic limit ϕ does not depend on $\vec{P}$, as indicated in (3.30). Our normalization is

$$\sum_{s_1s_2} \int d^3p\, |\phi_{\alpha\lambda}(\vec{p}s_1s_2)|^2 = 1 .$$

Expressions similar to (3.29) and (3.30) define the $c\bar{c}$ states; their wave functions are $\psi_n(\vec{k}s_1s_2)$, where n is shorthand for the quantum numbers $(nJLM)$.

The decay amplitudes are found by taking appropriate matrix elements of H_I:

$$\langle C_1(\vec{P}_1\lambda_1)\bar{C}_2(\vec{P}_2\lambda_2)|H_I|\psi_n\rangle , \quad (3.31)$$

where ψ_n is understood to be at rest. In evaluating (3.31), the field operators in the expression (3.2) for H_I are reduced to their nonrelativistic limits. After a rather lengthy calculation one finds

$$\langle C_1(\vec{P}\lambda_1)\bar{C}_2(\vec{P}'\lambda_2)|H_I|\psi_n\rangle = -i(2\pi)^{-3/2}\delta^3(\vec{p}+\vec{p}')3^{-1/2}A_{12}(\vec{P}\lambda_1\lambda_2;n) , \quad (3.32)$$

where

$$A_{12}(\vec{P}\lambda_1\lambda_2;n) = \frac{1}{m_q} \sum_{\{s\}} \int d^3x\, d^3y [\chi^\dagger(s_2')\vec{\sigma}\cdot\hat{x}\chi(-s_1')] \frac{dV(|\vec{x}|)}{d|\vec{x}|} \phi_1^*(\vec{x}s_1s_1')\phi_2^*(\vec{x}-\vec{y}, s_2s_2')\psi_n(\vec{y}s_1s_2)e^{-i\mu_c\vec{P}\cdot\vec{y}} , \quad (3.33)$$

where $\mu_c = m_c/(m_c+m_q)$, $\chi^\dagger, \chi$ are two-component spinors, and $\phi_i(\vec{x}ss')$, $\psi_n(\vec{y}ss')$ are the coordinate-space counterparts of the previously defined wave functions. The expression $(\chi^\dagger\vec{\sigma}\cdot\hat{x}\chi)$ describes the spin structure of the produced $q\bar{q}$ pair; it is a pseudoscalar because in our model the pair is created at zero separation. The factor $(m_q)^{-1}$ arises from the nonrelativistic reduction, and produces an explicit suppression of decays involving the production of heavy quarks. Whether this m_q dependence is realistic for the light (u,d,s) quarks is, of course, open to doubt.

Here we confine ourselves to S-wave charmed mesons (i.e., D, D^*, F, F^*). The P-wave case is rather more complex, and is discussed in Appendix D. For S-wave states, the ϕ_i are then simply products of a spherically symmetric function $\phi_i(|\vec{x}|)$, and a two-body spin function. The same is true for S-wave $c\bar{c}$ states. For P- and D-wave $c\bar{c}$ states, however, one must first construct states of good J from orbital and spin functions. This being done, one carries out the spin

sum in (3.33) and finds

$$A_{12}=a^{-2}\int d^3x\, d^3y Q_{LJM}(J_1\lambda_1 J_2\lambda_2;\hat{x},\hat{y}) \times \phi_1^*(|\vec{x}|)\phi_2^*(|\vec{x}-\vec{y}|)R_{nL}(|\vec{y}|)e^{-i\mu_c\vec{P}\cdot\vec{y}}, \tag{3.34}$$

where LJM are the usual angular momentum quantum numbers of ψ_n, R_{nL} its radial wave function, and J_1 and J_2 the spins of C_1 and $\bar{C}_2$. We have suppressed the total spin S of the $c\bar{c}$ system, for it is determined by the parity; we shall do this henceforth. As was mentioned in Sec. III B, we have for simplicity ignored in (3.34) all effects of the Coulombic term of the potential both in H_I and in the wave functions.

Q_{LJM} is a homogeneous polynomial of the Lth degree in $\hat{y}$, and of the first degree in $\hat{x}$. It is therefore only necessary to evaluate (3.34) with $Q=\hat{x}$; integrals with more complicated Q's can then be found by differentiating with respect to $\vec{P}$. As we are only concerned with ground-state charmed mesons here, it is both an excellent and convenient approximation to replace ϕ_i in (3.34) by Gaussians. Thus we must evaluate integrals of the form

$$\vec{K}\equiv\int d^3x\, d^3y\hat{x}e^{-\beta\vec{x}^2}e^{-\beta(\vec{x}-\vec{y})^2}R_{nL}(|\vec{y}|)e^{-i\mu_c\vec{P}\cdot\vec{y}}, \tag{3.35}$$

where

$$\beta=\frac{1}{2a^2}\left(\frac{4\mu a}{3\sqrt{\pi}}\right)^{2/3}. \tag{3.36}$$

For this purpose let us define

$$I^l_{nL}(P)=\int_0^\infty dt\,\Phi(t)R_{nL}(t\beta^{-1/2})j_l(\mu_c\beta^{-1/2}Pt), \tag{3.37}$$
$$\Phi(t)=te^{-t^2}+(\pi/2)^{1/2}(t^2-1)e^{-t^2/2}\,\mathrm{erf}(t/\sqrt{2}),$$

where j_l and erf are spherical Bessel and error functions. Then (3.35) becomes

$$\vec{K}=i\mu_c^{-1}\beta^{-5/2}\frac{\partial}{\partial\vec{P}}I^0_{nL}(P). \tag{3.38}$$

All terms in (3.34) can be similarly reduced to the I^l_{nL}, polynomials in $\hat{P}$, and polarization tensors for ψ_n, C_1, and $\bar{C}_2$. Further details are given in Appendix D.

We have evaluated I^l_{nL} numerically. Figure 3 shows the function I^1_{n0} for the decay of $n\,^3S_1$ states of charmonium into a $D\bar{D}$ pair or an $F\bar{F}$ pair as a function of the momentum of the decay product. The P- and F-wave integrals, I^1_{n2} and I^3_{n2}, for charmonium D states are shown in Fig. 4. for an outgoing $D\bar{D}$ pair and $n=1,2$. The parameters used in these calculations are the "renormalized" values.

The most striking features of these integrals are the rapid dropoff for large momentum P and the existence of nodes as discussed in Sec. III A. They are therefore sizeable only for the low-energy region ($P^2/2M\lesssim 0.5$ GeV), and have significant oscillations in this range. These features are crucial in understanding the behavior of ΔR, as well as the exclusive charmed-meson channels discussed in the second paper of this series.

The integrals I^l_{nL} depend on m_c, m_q, a, and P through the combinations β and $\mu_c P\beta^{-1/2}$ in a complicated manner. Comparison of the amplitudes for $F\bar{F}$ and $D\bar{D}$ production in Fig. 3 give some measure of dependence on the light quark mass for fixed a and m_c.

We now turn to the coupling matrix Ω_{nm}. Comparing (3.23) and (3.32), we see that the absorptive part of Ω_{nm} is proportional to

$$\frac{1}{2J+1}\sum_{M\lambda_1\lambda_2}\int d\hat{p}\,A^*_{12}(\vec{P}\lambda_1\lambda_2;nLJM) \times A_{12}(\vec{P}\lambda_1\lambda_2;mL'JM). \tag{3.39}$$

By virtue of (3.34)–(3.38), this can be reduced to a quadratic form in the $I^l_{nL}(P)$. The complete equation for Ω_{nm} is then

$$\Omega_{nL,mL'}(W)=\sum_i\int_0^\infty P^2dP\,\frac{H^i_{nL,mL'}(P)}{W-E_1(P)-E_2(P)+i0}, \tag{3.40}$$

with

$$H^i_{nL,mL'}(P)=f^2\sum_l C(JLL';l)I^l_{nL}(P)\,I^l_{mL'}(P), \tag{3.41}$$

where i labels the decay channel (e.g., $D\bar{D}, F\bar{F}^*$). The constant f^2 is defined by

$$f^2=\tfrac{2}{3}(m_q a^2\beta^{3/2}\pi)^{-2}=\frac{3}{\pi}\left(m_q\frac{m_cm_q}{m_c+m_q}\right)^2, \quad q=u,\ d,\ \text{or}\ s, \tag{3.42}$$

and the C's are combinations of 3-j and 6-j symbols. The dependence of $E_{1,2}(P)$ and f^2 on the channel index i is suppressed for simplicity. For more details see Appendix D.

The matrix $\Omega_{nL,mL'}$ only connects $c\bar{c}$ states having the same J^{PC}. Note also that insofar as we stick to the basic interaction (3.2) for all flavors of quarks, its spin-independent nature implies that the matrix $\Omega_{nL,mL'}$ is diagonal in L when all final spin states within the same $c\bar{q}$ (and $\bar{c}q$) multiplet are included. This is obvious from (D26). It is instructive, however, to examine some simple cases. Consider, for example, final states containing $D\bar{D}$, $D\bar{D}^*$, $D^*\bar{D}$, and $D^*\bar{D}^*$

pairs. Then we have

$$H^i_{n0,\,m2}(P) \propto \begin{pmatrix} -\sqrt{2}/3 \\ 2\sqrt{2}/3 \\ -\sqrt{2}/3 \end{pmatrix} I^1_{n0}(P)\, I^1_{m2}(P)$$

$$\text{for } i = \begin{pmatrix} 1:\ D\bar{D} \\ 2:\ D\bar{D}^* + D^*\bar{D} \\ 3:\ D^*\bar{D}^* \end{pmatrix} . \qquad (3.43)$$

In fact, with $m(D) = m(D^*)$ as required by a spin-independent V_0, $E^i_1(P)$, and $E^i_2(P)$ are independent of i, and the terms in the sum

$$\sum_{i=1}^{3} \frac{H^i_{n0,\,m2}(P)}{W - E^i_1(P) - E^i_2(P)}$$

cancel each other leading to a vanishing $\Omega_{n0,\,m2}(W)$.

This picture is obviously too crude to describe the charm threshold region where, in particular, the mass difference between D and D^* cannot be ignored. Since the calculation of charmed-meson masses is outside the domain of validity of (3.2), we treat these masses as external parameters. Thus we describe the charmonium system making use of the observed or estimated masses of

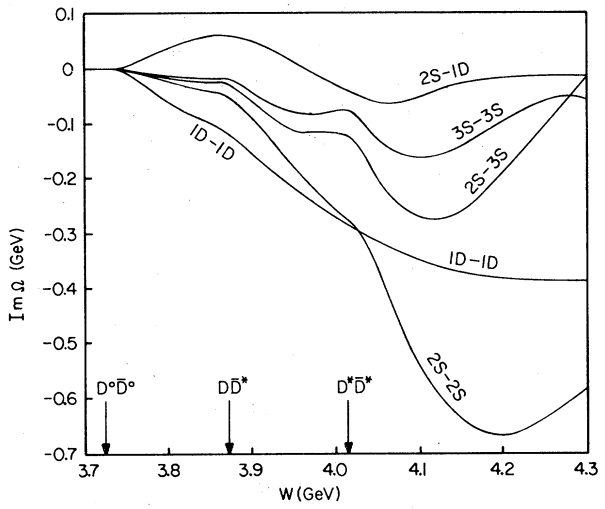

FIG. 7. Absorptive part of the effective $c\bar{c}$ interaction Ω. The thresholds for decay into nonstrange charmed mesons are shown. The $2S$-$1D$ element is responsible for the coupling between $\psi(3772)$ and the e^+e^- channel. In this figure the light-quark masses are the same as in Figs. 3 and 4, but $m_c = 1.45$ GeV and $a = 1.99$ GeV^{-1}. This change of parameters is brought about by the "renormalization" that must be done so that the ψ'-ψ mass difference agrees with the observed value *after* coupling to closed decay channels is incorporated. Meson masses are 1.863, 1.868, 2.006, 2.008, 1.995, and 2.135 GeV for D^0, D^+, D^{0*}, D^{+*}, F, and F^*, respectively.

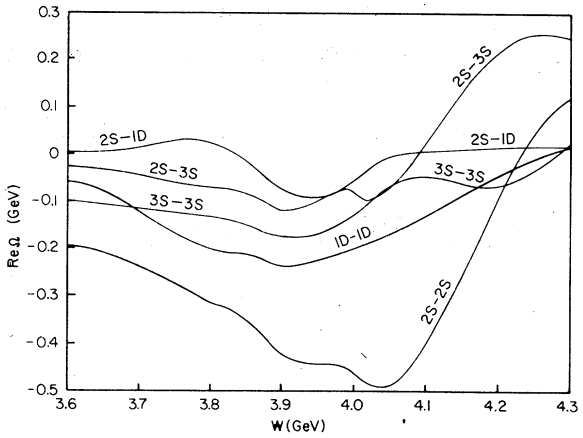

FIG. 8. Dispersive part of the effective $c\bar{c}$ interaction Ω; the latter is defined by Eqs. (3.22) and (3.23). Decay products included are all allowed two-body combinations of D, D^*, F, and F^*. These curves are obtained from those in Fig. 7 by the dispersion relation (3.40).

charmed mesons.

An important consequence of this procedure is that the cancellation mechanism illustrated by (3.43) no longer works and $\Omega_{nL,\,mL'}$ is generally nonvanishing for $L \neq L'$. In particular, this mechanism induces a strong S-D mixing between $2\,^3S_1$ and $1\,^3D_1$ charmonium states,[10,13] as we shall discuss in greater detail in Part II.

Some of the matrix elements of Ω evaluated numerically for the energy range 3.6–4.3 GeV are shown in Figs. 7 and 8. A strong and complicated energy dependence of Ω is evident, as well as the S-D mixing just referred to.

G. Exclusive channels

In order to understand the structure of ΔR, it is useful to express it as a sum of exclusive channel contributions. For this purpose let us rewrite (3.11) as

$$\Delta R(W) = -\frac{8}{W^2} \sum_{nm} \psi_{n0}(0)\psi_{m0}(0) \times \mathrm{Im}\langle n0 | \mathcal{G}(W + i0) | m0 \rangle , \qquad (3.44)$$

where $|m0\rangle$ is a $c\bar{c}$ 1^{--} state with $L = 0$ and principal quantum number m; $S = J = 1$ throughout, and therefore is suppressed.

Since $\mathcal{G}$ is symmetric and $G = G^\dagger$, we obtain from (3.18) and (3.22),

$$\mathcal{G} - \mathcal{G}^\dagger = \mathcal{G}^\dagger(\Omega - \Omega^\dagger)\mathcal{G} . \qquad (3.45)$$

On the other hand we have

$$\frac{1}{2i}(\Omega - \Omega^\dagger) = -\pi \sum_i H^i(P)\, \frac{P}{W}\, E_1 E_2 \qquad (3.46)$$

from (3.40). Returning to (3.44), we thus see

that the contribution of channel i is

$$R_i(W) = \frac{8\pi}{W^3} P_i E_1 E_2 \sum_{nm} \psi_{n0}(0) \langle n0 | \mathcal{G}^\dagger H^i \mathcal{G} | m0 \rangle \psi_{m0}(0) . \tag{3.47}$$

A more explicit form for the exclusive channel ratio R_i can be obtained by substituting (3.41) into (3.47). For instance, for the three channels cited in (3.43), we have

$$\begin{pmatrix} R_1 \\ R_2 \\ R_3 \end{pmatrix} = \frac{32\pi^2}{W^3} P_i E_1 E_2 f^2 \sum_{m,n} \sum_{m',n'} \psi_{m0}(0) \Bigg\{ \mathcal{G}^*_{m0,n0} \begin{pmatrix} \frac{1}{3} \\ \frac{4}{3} \\ \frac{7}{3} \end{pmatrix} I^1_{n0}(P_i) I^1_{n'0}(P_i) \mathcal{G}_{n'0,m'0}$$
$$+ \mathcal{G}^*_{m0,n2} \begin{pmatrix} -\sqrt{2}/3 \\ 2\sqrt{2}/3 \\ -\sqrt{2}/3 \end{pmatrix} I^1_{n2}(P_i) I^1_{n'0}(P_i) \mathcal{G}_{n'0,m'0} + \text{c.c.}$$
$$+ \mathcal{G}^*_{m0,n2} \left[\begin{pmatrix} \frac{2}{3} \\ \frac{2}{3} \\ \frac{4}{15} \end{pmatrix} I^1_{n2}(P_i) I^1_{n'2}(P_i) + \begin{pmatrix} 0 \\ 0 \\ \frac{12}{5} \end{pmatrix} I^3_{n2}(P_i) I^3_{n'2}(P_i) \right] \mathcal{G}_{n'2,m'0} \Bigg\} \psi_{m'0}(0) , \tag{3.48}$$

where the summation is over the radial quantum numbers of the 1^{--} charmonium states.

Two important features of R_i are clear from this formula. First, the $n\,^3D_1$ $c\bar{c}$ states do contribute to (3.47) and (3.44) as intermediate states; and second, the influence on R_i of channels other than the ith channel is fully incorporated into (3.47) through $\mathcal{G}$.

H. Leptonic widths and radiative decays

The influence on bound states of couplings to closed decay channels may now be studied. Let $|\alpha JM\rangle$ be a bound eigenstate; in the resolvent $(z-H)^{-1}$ it will appear as an isolated pole at $z = E_{\alpha J}$. Within our approximation scheme we have

$$|\alpha JM\rangle = \sum_{nL} a^{\alpha J}_{nL} |\psi; nL\, JM\rangle + \sum_i \sum_{\lambda_1\lambda_2} \int d^3p\, b^{\alpha J}_{i\lambda_1\lambda_2}(\vec{p}) |C; i\vec{p}\lambda_1\lambda_2 JM\rangle . \tag{3.49}$$

Here $|\psi; \cdots\rangle$ and $|C; \cdots\rangle$ are, respectively, states in the $c\bar{c}$ and decay sectors in the absence of decay couplings (i.e., eigenstates of H_ψ and H_C). As before, i labels the decay channel (e.g., $F\bar{F}^*$), λ_1, λ_2 are helicities of the charmed mesons, and $\vec{p}$ is their relative momentum.

In the notation of (3.44), the $c\bar{c}$ amplitudes in (3.49) are found from the residue of $\mathcal{G}^J(z)$ at $E_{\alpha J}$,

$$a^{\alpha J}_{nL}\, a^{\alpha J *}_{n'L'} = \lim_{z \to E_{\alpha J}} (z - E_{\alpha J}) \langle nL | \mathcal{G}^J(z) | n'L' \rangle , \tag{3.50}$$

where $\mathcal{G}^J$ is the part of $\mathcal{G}$ corresponding to fixed J (and S). To obtain the b amplitudes, we must consider matrix elements of $(z-H)^{-1}$ that connect the $c\bar{c}$ and decay sectors. Using (3.17) we have

$$\sum_\alpha (z - E_{\alpha J})^{-1} \langle C; i\vec{p}\lambda_1\lambda_2 JM | \alpha JM \rangle \langle \alpha JM | \psi; nL\, JM \rangle$$
$$= [z - E_1(p) - E_2(p)]^{-1} \times \sum_{n'L'} \langle C; i\vec{p}\lambda_1\lambda_2 J | H_I | \psi; n'L'J \rangle \langle n'L' | \mathcal{G}^J | nL \rangle .$$

Everything on the right-hand side of this formula is known. Hence

$$b^{\alpha J}_{i\lambda_1\lambda_2}(\vec{p})\, a^{\alpha J}_{nL} = \lim_{z \to E_{\alpha J}} (z - E_{\alpha J}) \times \frac{\langle C; i\vec{p}\lambda_1\lambda_2 J | H_I \mathcal{G} | \psi; nL\, J \rangle}{z - E_1(p) - E_2(p)} . \tag{3.51}$$

This completes our determination of the state vector (3.49).

The leptonic width of any 1^{--} state is then the obvious generalization of (2.2),

$$\Gamma(\psi_\alpha \to l\bar{l}) = \frac{16\pi e_c^{\,2} \alpha^2}{M_\alpha^{\,2}} \left| \sum_n a^{\alpha 1}_{n0} \psi_n(0) \right|^2 . \tag{3.52}$$

Since this is a coherent superposition of "naive" states, it is difficult to gain an intuitive understanding of the modifications of the leptonic widths produced by coupling to decay channels.

To evaluate radiative rates we need

$$\langle \alpha JM | \vec{j} | \alpha' J' M' \rangle , \tag{3.53}$$

where $\vec{j}$ is the quark electromagnetic current. For brevity we shall write (3.53) as $\vec{j}_{\alpha\alpha'}$. Since the states in (3.53) have the structure of (3.49), $\vec{j}_{\alpha\alpha'}$ is the sum of three terms: (i) a matrix element $\vec{j}^{\psi}_{\alpha\alpha'}$ in the $c\bar{c}$ sector; (ii) a matrix element $\vec{j}^{C}_{\alpha\alpha'}$ in the decay sector; and (iii) a cross term $\vec{j}^{X}_{\alpha\alpha'}$. The first two terms have an obvious physical significance. The third arises because $\vec{j}$ itself can create or destroy a $q\bar{q}$ pair, and thereby cause transitions between the two sectors.

At first sight one might think that these pair terms in $\vec{j}$ are manifestly negligible in a nonrelativistic model such as ours, and that $\vec{j}^{X}_{\alpha\alpha'}$ can be discarded without further thought. This is not so. The pair terms occur in the same (first) order as the conventional terms $\vec{j}^{\psi}_{\alpha\alpha'}$ and $\vec{j}^{C}_{\alpha\alpha'}$, and thus carry no suppressing energy denominators. It turns out, however, that $\vec{j}^{X}_{\alpha\alpha'}$ provides only minor contributions to transition rates. A summary of the rather involved calculation of $\vec{j}^{X}_{\alpha\alpha'}$ can be found in Appendix F.

The evaluation of the $\vec{j}^{\psi}_{\alpha\alpha'}$ is a straightforward generalization of what was reported in Sec. IID:

$$\vec{j}^{\psi}_{\alpha\alpha'} = \sum_{\substack{nn' \\ LL'}} a^{\alpha J *}_{nL} a^{\alpha' J'}_{n' L'} \langle \psi; nLJM | \vec{j} | \psi; n'L'J'M' \rangle . \tag{3.54}$$

The $E1$ matrix elements appearing in this sum are to be found in Appendix A.

For $E1$ transitions in the long-wavelength limit, the decay-sector element $\vec{j}^{C}_{\alpha\alpha'}$ is, in principle, very simple. The state $|C;\cdots\rangle$ in (3.49) can be treated as if it contained two structureless particles (mesons) that are either singly charged, or neutral. All effects arising from the meson magnetic moments or transition moments such as $D^* \to D\gamma$ do not contribute to these $E1$ transitions. Thus the basic matrix element is

$$\langle C_\alpha(\vec{p}\lambda) | \vec{j} | C_\beta(\vec{p}'\lambda') \rangle = \delta_{\alpha\beta}\delta_{\lambda\lambda'} \frac{e_\alpha}{(2\pi)^3} \frac{\vec{p}}{m_\alpha} \tag{3.55}$$

in the notation of (3.29). The two-body state in (3.49) is related to those appearing in (3.55) by the well-known formula of Jacob and Wick,

$$|C;\vec{p}\lambda_1\lambda_2 JM\rangle = \frac{2J+1}{4\pi} \int d\hat{p}\, D^J_{M,\lambda_1-\lambda_2}(\hat{p}) \times |C_1(\vec{p}\lambda_1)\overline{C}_2(-\vec{p}\lambda_2)\rangle .$$

As we have already shown how to determine the coefficients b in (3.49), all the ingredients for the evaluation of $\vec{j}^{C}_{\alpha\alpha'}$ are now at hand. Nevertheless, the final formulas are complex and their derivation involves a good deal of angular momentum manipulation. These details are summarized in Appendix E.

I. Meson-meson scattering

Scattering amplitudes such as $D\bar{D}^* \to F\bar{F}$ are not about to be measured. Nevertheless, we wish to point out that our techniques automatically provide an S matrix for such processes that is guaranteed to be unitary, and which incorporates those s-channel singularities that one would expect to dominate in the low-energy regime. As we hope that these calculations will stimulate similar work in the "old" spectroscopy, where scattering amplitudes are measured, we briefly indicate how to extract such amplitudes.

As explained in Sec. III D, we ignore "final-state" interactions between charmed mesons, or t-channel exchanges. These are expected to produce slow modulations of the rapidly varying amplitudes arising from the s-channel $c\bar{c}$ resonances that we do retain. The scattering amplitude is then

$$\langle \vec{p}_1\vec{p}_2 | T(z) | \vec{p}_1'\vec{p}_2' \rangle = \sum \langle \vec{p}_1\vec{p}_2 | U | nLSJM \rangle \times \langle nL | \mathcal{G}^{SJ}(z) | n'L' \rangle \times \langle n'L'SJM | U^\dagger | \vec{p}_1'\vec{p}_2' \rangle , \tag{3.56}$$

where, for simplicity, we are considering spinless mesons (i.e., $D\bar{D}$ or $F\bar{F}$ scattering). $\mathcal{G}^{SJ}$ is the part of $\mathcal{G}$ corresponding to fixed S and J. Consider first S-wave scattering. The intermediate $c\bar{c}$ states then have $L=S=1$, $J=0$ (i.e., $^3P_0$), and the matrix elements of U are of the form

$$\langle \vec{p}_1\vec{p}_2 | U | nS=L=1J=0 \rangle = \delta^3(\vec{p}_1+\vec{p}_2) \frac{D_n(W)}{(E_1E_2)^{1/2}} , \tag{3.57}$$

where $W = E_1 + E_2$, and the on-shell amplitude is

$$\langle \vec{p}_1\vec{p}_2 | T | \vec{p}_1'\vec{p}_2' \rangle = \delta^3(\vec{p}_1+\vec{p}_2-\vec{p}_1'-\vec{p}_2') \frac{4}{W^2} \times \sum_{nn'} D_n(W)\mathcal{G}^{10}_{nn'}(W) D_{n'}(W) . \tag{3.58}$$

Obviously the width matrix $\Gamma_{nn'}$, defined as

$$-i\Gamma_{nn'}(W) = \mathrm{Disc}\ \Omega_{nn'}(W) ,$$

is also bilinear in the $D_n(W)$. Its detailed form

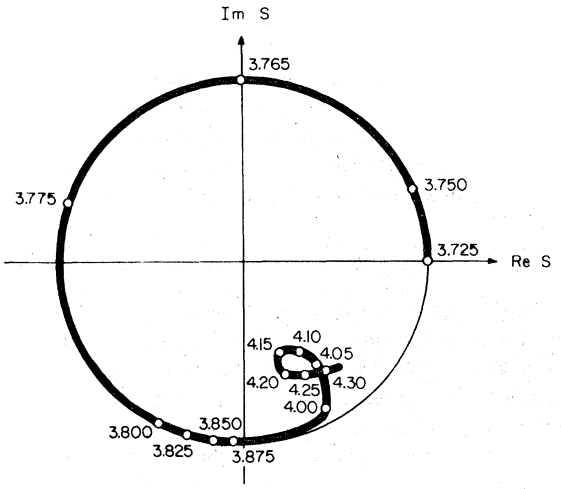

FIG. 9. Argand plot of the $D\bar{D}$ S matrix in the 1^{--} state. The rather narrow elastic $^3D_1$ resonance ψ (3772) is clearly in evidence, as is an inelastic resonance at ~4.15 GeV due to the $3\,^3S$ $c\bar{c}$ state. The parameters are the same as in Figs. 7 and 8.

is found by substituting (3.58) into (3.23):

$$\Gamma_{nn'} = 8\pi^2(p/W)D_n(W)D_{n'}(W)\,.$$

It now only remains to extract the partial-wave amplitude from (3.58). The final result for the phase shift is

$$e^{2i\delta} = 1 - \mathrm{Tr}\,\Gamma\mathcal{G}\,. \tag{3.59}$$

This expression also applies to other partial waves. Figure 9 shows $e^{2i\delta}$ for $D\bar{D}$ scattering in the 1^{--} partial wave from threshold to 4.3 GeV; the $^3D_1[\psi(3772)]$ and $3\,^3S$ resonances are clearly visible.

IV. CONCLUSION

We have shown that one can generalize the "naive" quark model, with its purely discrete spectrum, to a more realistic model that incorporates the important hadronic decay phenomenon. Though this generalized model still rests on a variety of drastic simplifications and approximations, it can be used to analyze a number of phenomena that are completely beyond the scope of the "naive" model.

Our formulation of the coupled-channel model has been tailor-made for the "new spectroscopy", and therefore relied rather heavily on the nonrelativistic approximation. A generalization of the model free of this restriction would be highly desirable as it would open up the vast store of data of "old hadronic" spectroscopy to a similar analysis.

While the formalism derived in Sec. III is based on a sequence of very plausible concepts and approximations, the solution of the equations in practical calculations requires further approximations that are not so well founded. In particular, we are, at this time, unable to handle a large enough set of decay channels to allow us to extend the calculations far above charm threshold. These more mundane matters will be discussed in detail in the second paper of this series.

ACKNOWLEDGMENTS

This work was supported in part by the National Science Foundation. The work of T.-M.Y. was also supported in part by the Sloan Foundation.

APPENDIX A. EIGENFUNCTIONS, EIGENVALUES, AND RADIATIVE MATRIX ELEMENTS IN THE $c\bar{c}$ SECTOR

In this appendix[34] we collect detailed information about the solutions of the Schrödinger equation

$$\left[\frac{d^2}{d\rho^2} - \frac{l(l+1)}{\rho^2} - \rho + \frac{\lambda}{\rho} + \zeta\right]u = 0\,. \tag{A1}$$

[see (2.8), (2.9), and (2.17) for notation]. u is normalized as in (2.10), and our phase convention is that $u_{nl} \to c_{nl}\rho^{l+1}$ as $\rho \to 0$, with $c_{nl} > 0$. We also define

$$\langle \rho^{-k} \rangle = \int_0^\infty \rho^{-k}[u(\rho)]^2 d\rho\,, \tag{A2}$$

$$\langle v^2 \rangle = \int_0^\infty [du/d\rho]^2 d\rho\,. \tag{A3}$$

As is seen from Fig. 2, only the $1S$ state is strongly affected by the Coulombic interaction for the range of λ of interest. We therefore provide a separate tabulation, Table I, for the $1S$ state which shows the λ dependence of the eigenvalue ζ_{10}, $\langle \rho^{-2} \rangle$, and $\langle v^2 \rangle$. Figure 10 shows $u_{10}(\rho)$ for

TABLE I. Dependence of the eigenvalue ζ_{10}, $\langle \rho^{-2} \rangle$, and $\langle v^2 \rangle$ for the $1S$ state on the Coulombic parameter λ.

λ	ζ_{10}	$\langle \rho^{-2} \rangle$	$\langle v^2 \rangle$
0.0	2.338 107	1.1218	0.7794
0.2	2.167 316	1.2494	0.8389
0.4	1.988 504	1.3942	0.9069
0.6	1.801 074	1.5583	0.9842
0.8	1.604 410	1.7435	1.0721
1.0	1.397 877	1.9519	1.1716
1.2	1.180 836	2.1856	1.2836
1.4	0.952 644	2.4466	1.4095
1.6	0.712 662	2.7366	1.5500
1.8	0.460 266	3.0898	1.7063

TABLE II. λ dependence of eigenvalues ζ and expectation values $\langle\rho^{-2}\rangle$ and $\langle v^2\rangle$.

	2S	3S	4S	1P	2P	1D	2D
$\zeta(0)$	4.0879	5.5206	6.7867	3.3613	4.8845	4.2482	5.6297
z_1	−0.5826	−0.4734	−0.4081	−0.5106	−0.4107	−0.3872	−0.3305
z_2	−0.0302	−0.0142	−0.0084	−0.0252	−0.0119	−0.0104	−0.0062
R_0^{-2}	0.8207	0.6953	0.6215	0.3141	0.2565	0.1679	0.1445
R_1^{-2}	0.2872	0.1954	0.1508	0.0582	0.0357	0.0176	0.0121
R_2^{-2}	0.0309	0.0085	0.0030	0.0093	0.0031	0.0015	0.0007
V_0	1.3626	1.8402	2.2622	0.4921	1.1151	0.4089	1.0097
V_1	0.1951	0.1593	0.1373	0.0516	0.0651	0.0231	0.0372
V_2	0.0293	0.0127	0.0072	0.0087	0.0062	0.0020	0.0023

several values of λ.

The other states have a much weaker λ dependence. For them the following interpolation formulas hold in the interval $0 \leq \lambda \leq 1.5$:

$$\zeta(\lambda) = \zeta(0) + z_1\lambda + z_2\lambda^2, \tag{A4}$$

$$\langle\rho^{-k}\rangle = R_0^{-k} + R_1^{-k}\lambda + R_2^{-k}\lambda^2, \tag{A5}$$

$$\langle v^2\rangle = V_0 + V_1\lambda + V_2\lambda^2. \tag{A6}$$

The coefficients in (A4)–(A6) are listed in Table II. Equation (A4) is accurate to one part in 10^4, (A5) and (A6) to one part in 10^3. Figure 11 shows the wave functions themselves when $\lambda = 0$.

Table III gives the first nonvanishing coefficients $a(n, l, \lambda)$ of the wave functions at the origin for some P and D state. These values are useful in estimating hadronic decay widths of charmonium states.

The $E1$ transitions involve the integrals

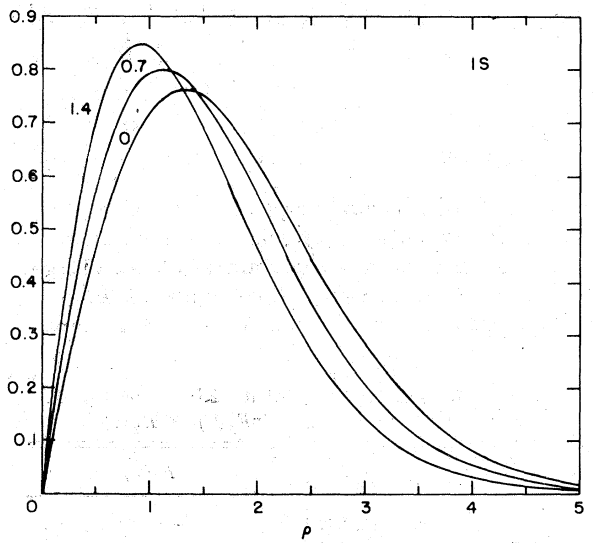

FIG. 10. The 1S wave function $u_{10}(\rho)$ for various values of the Coulombic parameter λ.

$$E_{if} = \frac{3}{2}\frac{1}{K}\int_0^\infty d\rho\, u_f(\rho)[K\rho j_0(K\rho) - j_1(K\rho)]u_i(\rho), \tag{A7}$$

where

$$K = \frac{ka}{2(m_c a)^{1/3}}. \tag{A8}$$

These are tabulated in Table IV for the case $K = 0$. The $K \neq 0$ correction for the $2S \to 1P$ transition is listed as a function of λ in Table V.

For hindered $M1$ transitions one needs the integrals

$$M_{fi}(K) = \int_0^\infty u_f(\rho)u_i(\rho)j_0(K\rho)d\rho. \tag{A9}$$

These are shown in Fig. 12 for the case $\lambda = 0$.

APPENDIX B. SUM RULES SPECIFIC TO LINEAR POTENTIALS

For purely linear potentials, the $E1$ transition matrix elements $\epsilon_{nL,n'L'}$ defined by

$$\epsilon_{nL,n'L'} = \int_0^\infty \rho d\rho\, u_{nL}(\rho)u_{n'L'}(\rho) \tag{B1}$$

satisfy a peculiar sum rule,

$$\sum_{n'=0}^{\infty} \epsilon_{nL,n'0} = 0. \tag{B2}$$

A similar sum rule holds for the integral

TABLE III. λ dependence of the first nonvanishing coefficients $|a(n, l, \lambda)|$ of the wave functions at the origin defined by $\psi_{nl}(\vec{r}) \sim a(n, l, \lambda)r^l Y_{lm}$ for $r \approx 0$.

	$\lvert a(n,l,\lambda)\rvert$			
λ	1P	2P	1D	2D
0.0	0.517	0.674	0.194	0.302
0.6	0.657	0.825	0.238	0.361
1.2	0.830	1.001	0.291	0.431
1.8	1.042	1.209	0.354	0.513

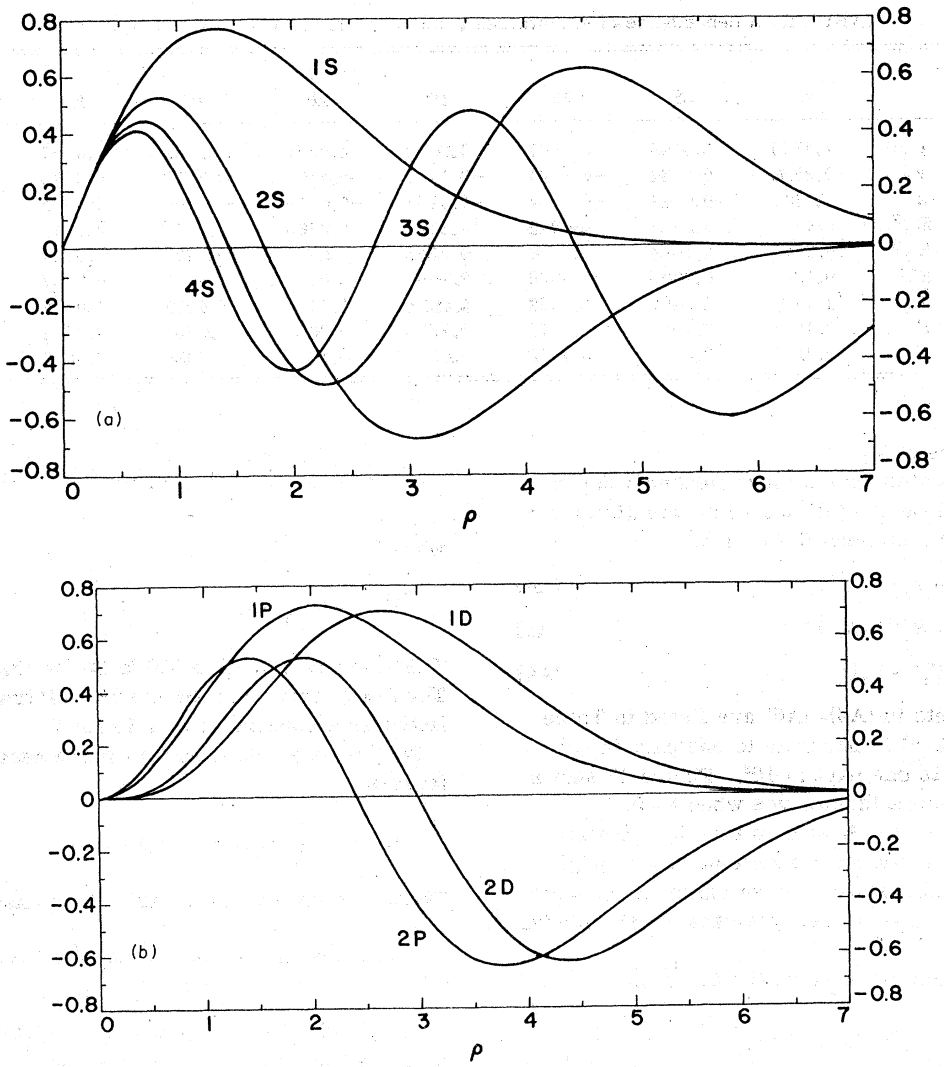

FIG. 11. (a) Wave functions for low-lying S states for the case $\lambda = 0$. (b) Wave functions for low-lying P and D states for the case $\lambda = 0$.

$$I^{l}_{\eta L}(p) = \int_0^\infty dt\, \Phi(t) j_l\left(\frac{\mu_c p}{\sqrt{\beta}}\, t\right) R_{nL}\left(\frac{t}{\sqrt{\beta}}\right),$$

which appears in the decay amplitude. In this case we have

TABLE IV. $E1$ matrix elements E_{if}.

λ		0	0.5	1.0	1.5
$1S$	$1P$	1.705	1.559	1.412	1.268
$2S$	$1P$	−1.646	−1.670	−1.686	−1.691
$3S$	$1P$	−0.043 43	−0.020 37	0.004 59	0.030 52
$1S$	$2P$	0.097 5	0.147 1	0.190 2	0.224 4
$2S$	$2P$	2.488	2.333	2.177	2.020
$3S$	$2P$	−2.488	−2.534	−2.573	−2.601
$1D$	$1P$	2.368	2.280	2.192	2.105
$1D$	$2P$	−1.758	−1.767	−1.774	−1.779

$$\sum_{n=0}^{\infty} I^{l}_{n0}(p) = 0. \tag{B3}$$

These sum rules provide a powerful check on the consistency of numerical work. It is seen from numerical results that $nP \to n'S$ amplitudes are large only for $n' = n$ and $n' = n+1$. The sum rule (B2) tells us that these two amplitudes are of the same

TABLE V. $K \neq 0$ correction for the $2S \to 1P$ transition as a function of λ, where $E(\lambda, K) = E_1(\lambda) - K^2 E_2(\lambda)$.

λ	$E_2(\lambda)$	$E_1(\lambda)$
0	−3.734	−1.646
0.7	−3.297	−1.677
1.4	−2.871	−1.691

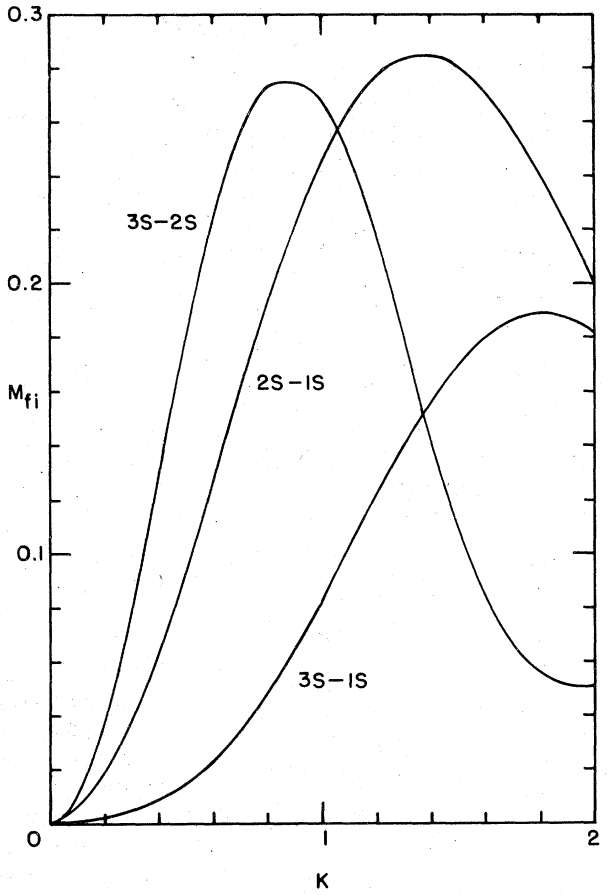

FIG. 12. Matrix elements for some hindered $M1$ transitions as functions of $K=(ka/2)(m_c a)^{-1/3}$ for the case $\lambda=0$.

order of magnitude and of opposite sign (see Table IV).

Proof of (B2): Consider the completeness relation for $L'=0$:

$$\sum_{n'=1}^{\infty} u_{n'0}(\rho)u_{n'0}(\rho') = \delta(\rho-\rho'). \tag{B4}$$

Differentiating this with respect to ρ', we obtain

$$\sum_{n'=1}^{\infty} u_{n'0}(\rho)\frac{d}{d\rho'}u_{n'0}(\rho') = \frac{d}{d\rho'}\delta(\rho-\rho')$$

$$= -\frac{d}{d\rho}\delta(\rho-\rho'). \tag{B5}$$

Now, *for linear potentials only*, we get

$$\frac{d}{d\rho'}u_{n'0}(\rho')\Big|_{\rho'=0} = c = \text{const. independent of } n'. \tag{B6}$$

From (B5) and (B6) we find

$$\sum_{n'=1}^{\infty} u_{n'0}(\rho) = -\frac{1}{c}\frac{d}{d\rho}\delta(\rho). \tag{B7}$$

Thus we obtain

$$\sum_{n'=1}^{\infty}\epsilon_{nL,n'0} = -\frac{1}{c}\int_0^{\infty}\rho d\rho\, u_{nL}(\rho)\frac{d}{d\rho}\delta(\rho)$$

$$= \frac{1}{c}u_{nL}(0+)$$

$$= 0 \tag{B8}$$

for $L=0,1,2,\ldots$, which proves (B2).

The sum rule (B3) can be derived by a similar argument. We have only to note that

$$u_{nL}(\rho) = \rho R_{nL}(\rho)$$

and

$$\Phi(t) \to \tfrac{2}{3}t^3$$

for $t\to 0$.

APPENDIX C. DERIVATION OF FORMULA (3.11)

In this appendix we derive the charm contribution to the ratio R in e^+e^- annihilation. The ratio ΔR due to charm is given by

$$\Delta R(W) = \frac{6\pi}{W^2}\rho_c(W), \tag{C1}$$

where $q^2=W^2$ and

$$-(g_{\mu\nu}q^2 - q_\mu q_\nu)\rho_c(W)$$

$$= \int d^4x\, e^{iqx}\langle 0|j_\mu(x)j_\nu(0)|0\rangle\Big|_{\text{charm}}. \tag{C2}$$

Thus our task is to calculate $\rho_c(W)$.

Since quarks are confined in our model, e^+e^- annihilation into hadrons proceeds through the production of spin-1 $c\bar{c}$ bound states. Let us first evaluate the matrix elements of the electromagnetic current j_μ between the vacuum and these bound states. Expanding the bound states as in (3.29), and expressing j_μ in terms of the quark creation and destruction operators, we find that

$$\langle n,\lambda|j_\mu(0)|0\rangle = \left[\frac{6}{(2\pi)^3}\right]^{1/2} e_c\epsilon_\mu(\lambda)\psi_n(0), \tag{C3}$$

where $|n,\lambda\rangle$ is the nth $c\bar{c}$ bound state at rest with polarization λ, $\epsilon_\mu(\lambda)$ is the polarization vector, and $\psi_n(0)$ is the spatial wave function at the origin. Since $\psi_n(0)$ vanishes for nonzero-orbital-angular-momentum states, only S states contribute to the matrix element (C3).

Next, let us introduce a phenomenological field, $\phi_{n\mu}(x)$, associated with each bound state $n\,^3S_1$. Then, using the matrix elements (C3) as coefficients, we can express the electromagnetic current j_μ as a linear combination of these fields:

$$j_\mu(x) = e_c\sqrt{6}\sum_\eta \psi_\eta(0)[\phi_{\eta\mu}(x) + \phi^\dagger_{\eta\mu}(x)]\,. \tag{C4}$$

The field operators $\phi_{\eta\mu}(x)$ satisfy the equal-time commutation relations

$$[\phi_{mi}(\vec{x}),\ \phi^\dagger_{nj}(\vec{x}')] = \delta_{mn}\delta_{ij}\delta^3(\vec{x}-\vec{x}')\,. \tag{C5}$$

Finally we define the retarded Green's function

$$\delta_{ij}\mathcal{G}_{mn}(q^0) = -\int d^4x\, e^{iq^0x^0} i\theta(x^0) \times \langle 0|\phi_{mi}(x)\phi^\dagger_{nj}(0)|0\rangle\,. \tag{C6}$$

Then from Eqs. (C2), (C4), and (C6) we readily obtain

$$\rho_c(W) = -12e_c^{\,2}\,\mathrm{Im}\left[\sum_m\sum_n \psi_m(0)\mathcal{G}_{mn}(W)\psi_n(0)\right]\,. \tag{C7}$$

Together with (C1) this is equivalent to (3.11) if $e_c^{\,2} = \frac{4}{9}$ is substituted. It is easy to verify that $\mathcal{G}_{mn}$ defined here is the submatrix of the resolvent introduced in Sec. III restricted to the S states.

APPENDIX D. DECAY AMPLITUDES AND RELATED QUANTITIES

We supply here some details of our treatment of decay amplitudes and related quantities.

We begin with the Fourier transform of the wave function $\phi_{\alpha\lambda}(\vec{p}, s_1s_2)$ defined in (3.29):

$$\phi_{\alpha\lambda}(\vec{x}, s_1s_2) = \int \frac{d^3p}{(2\pi)^{3/2}}\, e^{i\vec{p}\cdot\vec{x}}\phi_{\alpha\lambda}(\vec{p}, s_1s_2)\,, \tag{D1}$$

which can be written as a product of radial and spin-angular wave functions,

$$\phi_{\alpha\lambda}(\vec{x}, s_1s_2) = \phi_\alpha(|\vec{x}|)\chi_{JMls}(s_1s_2, \hat{x})\,. \tag{D2}$$

They satisfy the normalization conditions

$$\int_0^\infty dr\, r^2\,|\phi_\alpha(r)|^2 = 1\,, \tag{D3}$$

$$\sum_{s_1s_2}\int d\Omega\,|\chi_{JMls}(s_1s_2, \hat{x})|^2 = 1\,. \tag{D4}$$

The function χ_{JMls} describes a state of total angular momentum J and its z-component M constructed by the standard procedure from the spherical harmonics $Y_{lm}(\hat{x})$ and the spin eigenfunctions

$$\chi_{s\lambda}(s_1s_2) = \frac{1}{\sqrt{2}}\,\chi^\dagger(s_1)\Gamma_{s\lambda}\chi(-s_2)\,. \tag{D5}$$

The matrix $\Gamma_{s\lambda}$ for a state of spin 0 is

$$\Gamma_{s\lambda} = 1, \tag{D6}$$

while that for a state of spin 1 and polarization λ is

$$\Gamma_{s\lambda} = \vec{\sigma}\cdot\vec{\epsilon}_\lambda, \tag{D7}$$

where $\vec{\epsilon}_\lambda$ is the polarization vector.

Let us first consider the amplitude (3.33) for the decay of a charmonium state into a pair of S-wave charmed mesons (D, D^*, F, and F^*). Following the discussion of Sec. III B, we shall ignore all effects of the Coulombic term both in the potential V and in the wave functions. Thus, in particular, we replace dV/dx by a a^{-2}. Then (3.33) can be rewritten as

$$A_{12}(\vec{P}\lambda_1\lambda_2; n) = \frac{1}{2m_q}\,\frac{1}{a^2}\sum_{m\lambda\mu}\langle JM|Lm, s\lambda\rangle S(J_1\lambda_1, J_2\lambda_2, s\lambda, \mu) \times \int d^3x\, d^3y\, \hat{x}_\mu Y_{lm}(\hat{y})\phi_1(|\vec{x}|)\phi_2(|\vec{x}-\vec{y}|)R_{nL}(|\vec{y}|)e^{-i\mu_c\vec{P}\cdot\vec{y}}\,, \tag{D8}$$

where R_{nL} is the radial part of the charmonium wave function $\psi_l(\vec{y})$ [see (E3)] and

$$S(J_1\lambda_1, J_2\lambda_2, s\lambda, \mu) = \tfrac{1}{2}\,\mathrm{Tr}(\sigma^\dagger_\mu\Gamma^\dagger_{J_1\lambda_1}\Gamma_{s\lambda}\,\Gamma^\dagger_{J_2\lambda_2})\,. \tag{D9}$$

The vector $\hat{x}_\mu$ has the components

$$\hat{x}_\pm = \mp\frac{1}{\sqrt{2}}\,(\hat{x}_1 \pm i\hat{x}_2)\,,\quad \hat{x}_0 = \hat{x}_3. \tag{D10}$$

The same applies to σ_μ. Approximating the wave functions ϕ_1 and ϕ_2 by the Gaussian trial functions

$$\phi_1(x) = \phi_2(x) = \left(\frac{2\beta_S}{\pi}\right)^{3/4} e^{-\beta_S x^2}\,, \tag{D11}$$

where β_S is determined by a variational calculation and is given by (3.36), we obtain

$$\int d^3x\,\hat{x}\phi_1(|\vec{x}|)\phi_2(|\vec{x}-\vec{y}|) = \hat{y}\,\frac{1}{\beta_S y^2}\left(\frac{2}{\pi}\right)^{1/2}\Phi(\sqrt{\beta_S}\,y)\,, \tag{D12}$$

with

$$\Phi(t)=te^{-t^2}+(t^2-1)e^{-t^2/2}\left(\frac{\pi}{2}\right)^{1/2}\operatorname{erf}\left(\frac{t}{\sqrt{2}}\right). \tag{D13}$$

Carrying out the angular integration over $\hat{y}$ we arrive at

$$A_{12}(\vec{P}\lambda_1\lambda_2,n)=\sum_{lm}B_{LJM}(sJ_1\lambda_1,J_2\lambda_2,lm)(-1)^l I^l_{nL}(P)Y_{lm}(\hat{P}), \tag{D14}$$

where

$$B_{LJM}(sJ_1\lambda_1,J_2\lambda_2,lm)=\frac{1}{m_q a^2}\left(\frac{16\pi}{\beta^3}\right)^{1/2}\sum_{M'm'\lambda}\left(\frac{2L+1}{2l+1}\right)^{1/2}\langle LsM'\lambda|JM\rangle\langle L100|l0\rangle$$
$$\times\langle L1M'm'|lm\rangle S(J_1\lambda_1,J_2\lambda_2,s\lambda,m'), \tag{D15}$$

and

$$I^l_{nL}(P)=\int_0^\infty dt\,\Phi(t)R_{nL}\left(\frac{t}{\sqrt{\beta}}\right)j_l\left(\frac{\mu_c Pt}{\sqrt{\beta}}\right). \tag{D16}$$

Substituting (D14) into Eq. (3.23), we obtain

$$\Omega^{J,s}_{nL,mL'}(W)=\sum_{J_1J_2}\int_0^\infty P^2dP\,\frac{H^{J,J_1J_2s}_{nL,mL'}(P)}{W-E_1(P)-E_2(P)+i0}, \tag{D17}$$

where

$$H^{J,J_1J_2s}_{nL,mL'}(P)=f^2\sum_l C(JJ_1J_2s,LL',l)I^l_{nL}(P)I^l_{mL'}(P), \tag{D18}$$

The coefficients C are determined by

$$3(2\pi)^3f^2C(JJ_1J_2s,LL',l)=\sum_m\sum_{\lambda_1\lambda_2}B^*_{LJM}(sJ_1\lambda_1J_2\lambda_2lm)B_{L'JM}(sJ_1\lambda_1J_2\lambda_2lm)$$
$$=\frac{1}{2J+1}\sum_{mM}\sum_{\lambda_1\lambda_2}B^*_{LJM}(sJ_1\lambda_1J_2\lambda_2lm)B_{L'JM}(sJ_1\lambda_1J_2\lambda_2lm), \tag{D19}$$

where the last line is a consequence of the independence of C on the magnetic quantum number M; we have also defined

$$f^2=\tfrac{2}{3}(m_q a^2\beta_S{}^{3/2}\pi)^{-2}=\frac{3}{\pi}\left(m_q\frac{m_cm_q}{m_c+m_q}\right)^2. \tag{D20}$$

The summation over various magnetic quantum numbers in Eq. (D19) can be carried out by a standard exercise in combining several angular momenta. The results involve 6-j symbols and are given below.

(1) $s=0$:

$$C=\delta_{LL'}\delta_{JL}|\langle L100|l0\rangle|^2B(J_1J_2), \tag{D21}$$

$$B(J_1J_2)=0 \quad \text{if } J_1=J_2=0,$$
$$B(J_1J_2)=1 \quad \text{if } J_1=1,\ J_2=0 \text{ or } J_1=0,\ J_2=1, \tag{D22}$$
$$B(J_1J_2)=2 \quad \text{if } J_1=J_2=1.$$

(2) $s=1$:

(i) $J_1=J_2=0$,

$$C=\delta_{Jl}\frac{[(2L+1)(2L'+1)]^{1/2}}{2J+1}\times\langle L100|J0\rangle\langle L'100|J0\rangle. \tag{D23}$$

(ii) $J_1=1$, $J_2=0$ or $J_1=0$, $J_2=1$,

$$C=[(2L+1)(2L'+1)]^{1/2}\langle L100|l0\rangle\langle L'100|l0\rangle\times\left[\frac{\delta_{LL'}}{2L+1}-\begin{Bmatrix}L & L & J\\ L' & 1 & l\end{Bmatrix}\right]. \tag{D24}$$

(iii) $J_1=J_2=1$,

$$C=[(2L+1)(2L'+1)]^{1/2}\langle L100|l0\rangle\langle L'100|l0\rangle\times\left[\frac{2\delta_{LL'}}{2L+1}+2\begin{Bmatrix}L & 1 & J\\ L' & 1 & l\end{Bmatrix}-\frac{\delta_{Jl}}{2J+1}\right]. \tag{D25}$$

Note that for $s=1$ the following relation holds,

$$\sum_{J_1J_2}C(JJ_1J_2s,LL',l)=4\delta_{LL'}|\langle L100|l0\rangle|^2. \tag{D26}$$

TABLE VI. Systematics for decays containing charmed P states. Here j_L is the total angular momentum of the light-quark constituent of D_P as seen in the rest frame of c.

Final state	Threshold behavior	Statistical factor
$D\bar{D}_{P_0}$	Forbidden	...
$D\bar{D}_{P_1}$ ($j_L=\frac{1}{2}$)	S-wave	$\frac{2}{3}$
$D^*\bar{D}_{P_0}$	S-wave	$\frac{2}{3}$
$D^*\bar{D}_{P_1}$ ($j_L=\frac{1}{2}$)	S-wave	$\frac{4}{3}$
$D\bar{D}_{P_2}$	D-wave	$\frac{2}{3}$
$D\bar{D}_{P_1}$ ($j_L=\frac{3}{2}$)	D-wave	$\frac{2}{3}$
$D^*\bar{D}_{P_1}$ ($j_L=\frac{3}{2}$)	D-wave	$\frac{4}{3}$
$D^*\bar{D}_{P_2}$	D-wave	$\frac{8}{3}$

This means that if one ignores the mass difference of the s-wave charmed mesons of different spins, then there is no mixing among states of different orbital angular momenta.

We have also considered the quasi-two-body decay of $(c\bar{c})$ bound states with the next lowest thresholds, decay into a ground-state charmed meson (D or D^*) and a P-state charmed meson[13] (D_{P_0}, D_{P_1}, D_{P_2}, or D_P).

A good approximation for the radial wave function of the P-state charmed mesons is given by

$$\phi_P(x) = N_P\, x e^{-\beta_P x^2}, \tag{D27}$$

where N_P is the normalization constant and β_P is obtained from a variational calculation. The explicit form of β_P is

$$\beta_P = \frac{1}{2a^2}\left(\frac{16\mu a}{15\sqrt{\pi}}\right)^{2/3}, \quad (\mu = \text{reduced mass}). \tag{D28}$$

Proceeding as before, we can calculate the various invariant decay amplitudes and finally the contribution to $\Omega(W)$ of each of these final states. The calculations are quite tedious; we record here only the results for the contribution to Ω.

Consider the decay $(c\bar{c})\ n^{2s+1}L_J$ into $(c\bar{q})\ 1^{2s_1+1}S_{J_1}$ and $(\bar{c}q)\ 1^{2s_2+1}P_{J_2}$; then the contribution of this final state to Ω is given by

$$\Omega^{(J,s)J_1(J_2,s_2)}_{nl_1ml_2}(W) = \int_0^\infty dP P^2 \frac{H^{(J,s)J_1(J_2,s_2)}_{nl_1ml_2}(P)}{W - E_1(P) - E_2(P)}, \tag{D29}$$

where

$$H^{(J,s)J_1(J_2,s_2)}_{nl_1ml_2}(P) = (f')^2 \sum_{\tilde{L}=0,1,2}\sum_{L'=0,2}\Bigg[\sum_{l_1'}[(2l_1+1)(2l_1'+1)(2J_2+1)(2\tilde{L}+1)]^{1/2}\langle 1100|l_1'0\rangle\langle l_1l_1'00|L'0\rangle\, \mathcal{J}^{l_1'L'}_{nl_1}(P)$$
$$\times \sum_{\bar{s}=0,1} 3(1+\bar{s})^{(J_1+s_2)/2}(-1)^{\bar{s}} \begin{Bmatrix} l_1' & \bar{s} & J_2 \\ s_2 & 1 & 1 \end{Bmatrix}\begin{Bmatrix} l_1' & \bar{s} & J_2 \\ \tilde{L} & L' & l_1 \end{Bmatrix}\begin{Bmatrix} l_1 & \bar{s} & \tilde{L} \\ J_1 & J & s \end{Bmatrix}\Bigg]$$
$$\times\Bigg[\sum_{l_2'}[(2l_2+1)(2l_2'+1)(2J_2+1)(2\tilde{L}+1)]^{1/2}\langle 1100|l_2'0\rangle\langle l_2l_2'00|L'0\rangle\, \mathcal{J}^{l_2'L'}_{ml_2}(P)$$
$$\times \sum_{\bar{s}'=0,1} 3(1+\bar{s}')^{(J_1+s_2)/2}(-1)^{\bar{s}'} \begin{Bmatrix} l_2' & \bar{s}' & J_2 \\ s_2 & 1 & 1 \end{Bmatrix}\begin{Bmatrix} l_2' & \bar{s}' & J_2 \\ \tilde{L} & L' & l_2 \end{Bmatrix}\begin{Bmatrix} l_2 & \bar{s}' & \tilde{L} \\ J_1 & J & s \end{Bmatrix}\Bigg], \tag{D30}$$

with

$$f' = \frac{2}{a^2}\frac{1}{2m_d}\left(\frac{2\beta_S}{\pi}\right)^{3/4}\frac{4}{\sqrt{3}}\left(\frac{8\beta_P^5}{\pi}\right)^{1/4}, \tag{D31}$$

$$\mathcal{J}^{l'L'}_{nl}(P) = \int_0^\infty dy\, y^2 \psi_{nl}(y) j_{l'}(\mu_c P y) A_{L'}(y), \tag{D32}$$

$$A_0(y) = \frac{1}{4(\beta_S+\beta_P)^2}\exp\left(-\frac{\beta_S\beta_P}{\beta_S+\beta_P}y^2\right)$$
$$\times\Bigg[-\exp\left(-\frac{\beta_S^2y^2}{\beta_S+\beta_P}\right) - \sqrt{\pi}\left(\frac{\beta_S}{(\beta_S+\beta_P)^{1/2}}y + \frac{(\beta_S+\beta_P)^{1/2}}{2\beta_S y}\right)\operatorname{erf}\left(\frac{\beta_S y}{(\beta_S+\beta_P)^{1/2}}\right)$$
$$-\frac{\beta_S}{\beta_P}\exp\left(-\frac{\beta_P^2y^2}{\beta_S+\beta_P}\right) + \sqrt{\pi}\left(\frac{(\beta_S+\beta_P)^{1/2}}{2\beta_P^2 y}(\beta_S+2\beta_P) - \frac{\beta_S}{(\beta_S+\beta_P)^{1/2}}y\right)\operatorname{erf}\left(\frac{\beta_P y}{(\beta_S+\beta_P)^{1/2}}\right)\Bigg], \tag{D33}$$

$$A_2(y) = \frac{1}{4(\beta_S+\beta_P)^2}\exp\left(-\frac{\beta_S\beta_P}{\beta_S+\beta_P}y^2\right)$$
$$\times\left\{\left(-1+\frac{3(\beta_S+\beta_P)}{2\beta_S^2y^2}\right)\exp\left(\frac{-\beta_S^2y^2}{\beta_S+\beta_P}\right)\right.$$
$$-\sqrt{\pi}\left(\frac{3}{4}\frac{(\beta_S+\beta_P)^{3/2}}{\beta_S^{3/2}y^3}-\frac{(\beta_S+\beta_P)^{1/2}}{\beta_Sy}+\frac{\beta_S}{(\beta_S+\beta_P)^{1/2}}y\right)\operatorname{erf}\left(\frac{\beta_Sy}{(\beta_S+\beta_P)^{1/2}}\right)$$
$$\left.+\sqrt{\pi}\left[\frac{3}{4}\frac{(\beta_S+\beta_P)^{3/2}}{\beta_P^3y^3}+\frac{(\beta_S+\beta_P)^{1/2}}{2\beta_Py}\left(\frac{\beta_S}{\beta_P}-1\right)-\frac{\beta_S}{(\beta_S+\beta_P)^{1/2}}y\right]\operatorname{erf}\left(\frac{\beta_Py}{(\beta_S+\beta_P)^{1/2}}\right)\right]. \tag{D34}$$
$$-\left(\frac{\beta_S}{\beta_P}+\frac{3}{2}\frac{\beta_S+\beta_P}{\beta_P^2y^2}\right)\exp\left(-\frac{\beta_P^2y^2}{\beta_S+\beta_P}\right)$$

In general, both S-wave and D-wave decays are possible. For the decays of a ${}^3S_1$ ($c\bar{c}$) state into D (or D^*) and a $\bar{D}_{P_J}$ the threshold behavior is shown in Table VI.

APPENDIX E. $\vec{j}^{\psi}_{\alpha\alpha'}$ AND $\vec{j}^{C}_{\alpha\alpha'}$ CONTRIBUTIONS TO ELECTRIC DIPOLE MATRIX ELEMENTS

The purpose of this and the following appendix is to derive explicit expressions for the various pieces of an $E1$ transition matrix element introduced in Sec. III H. In this appendix we will present results for $\vec{j}^{\psi}_{\alpha\alpha'}$ and $\vec{j}^{C}_{\alpha\alpha'}$: the matrix element of the electric dipole operator in the $c\bar{c}$ sector and the charmed-meson sector, respectively. In the $c\bar{c}$ sector, the constituents are quarks whose wave function is an eigenfunction of a nonrelativistic Schrödinger equation. (As in Appendix D, we ignore all effects of the Coulombic term both in the potential V and in the wave functions.) In the charmed-meson sector, on the other hand, the mesons are the constituents and the wave functions are given essentially by the decay amplitudes computed in Appendix D. Thus we find it convenient to work in coordinate space when computing $\vec{j}^{\psi}_{\alpha\alpha'}$ but in momentum space when computing $\vec{j}^{C}_{\alpha\alpha'}$.

As is seen from (3.54), $\vec{j}^{\psi}_{\alpha\alpha'}$ is given by

$$\vec{j}^{\psi}_{\alpha\alpha'} = \sum_{nn'}\sum_{LL'} a^{\alpha J*}_{nL}a^{\alpha' J'}_{n'L'}\langle\psi; nLJM|\vec{j}|\psi; n'L'J'M'\rangle\,, \tag{E1}$$

where the coefficients $a^{\alpha J}_{nL}$ are given by (3.50). In the electric dipole approximation we have

$$\langle\psi; nLJM|\vec{j}|\psi; n'L'J'M'\rangle = -i\frac{k}{(2\pi)^3}e_c\sum_{s_1s_2}\int d^3x\,\psi^*_{nLJM}(\vec{x}, s_1s_2)\vec{x}\psi_{n'L'J'M'}(\vec{x}, s_1s_2)\,. \tag{E2}$$

The wave function ψ can be written as

$$\psi_{nLJM}(\vec{x}, s_1s_2) = R_{nL}(r)\chi_{JML}(\hat{x}, s_1s_2)\,, \tag{E3}$$

with

$$\chi_{JML}(\hat{x}, s_1s_2) = \sum_{m\mu}\langle L, s=1, m\mu|JM\rangle\frac{1}{\sqrt{2}}\chi^\dagger(s_1)\sigma_\mu\chi(-s_2)Y_{Lm}(\hat{x})\,, \tag{E4}$$

where we have restricted ourselves to triplet spin states. Substituting (E2)–(E4) in (E1) and carrying out spin sums and angular integrations, we find

$$\vec{j}^{\psi}_{\alpha\alpha'} = (-ik)\frac{a}{(m_ca)^{1/3}}\frac{e_c}{(2\pi)^3}\frac{1}{\sqrt{3}}(-1)^{M'}[(2J+1)(2J'+1)]^{1/2}\sum_\mu\vec{\xi}_\mu\begin{pmatrix}J' & J & 1\\ -M' & M & \mu\end{pmatrix}$$
$$\times\sum_{nn'}\sum_{LL'}a^{\alpha J*}_{nL}a^{\alpha' J'}_{n'L'}\langle 10|L'L00\rangle[(2L+1)(2L'+1)]^{1/2}\begin{Bmatrix}J' & J & 1\\ L & L' & 1\end{Bmatrix}E_{nL,n'L'}\,, \tag{E5}$$

where $E_{nL,n'L'}$ is the dimensionless dipole matrix element defined by (2.22). We have also introduced the vectors

$$\vec{\xi}_{\pm1} = \mp\frac{1}{\sqrt{2}}(1, \pm i, 0)\quad \vec{\xi}_0 = (0, 0, 1)\,. \tag{E6}$$

We now turn to the calculation of $\vec{j}^{C}_{\alpha\alpha'}$. In the notation of Sec. III H we write

$$P_C|\alpha JM\rangle = \sum_i\sum_{\lambda_1\lambda_2}\int d^3p\,b^{\alpha J}_{i\lambda_1\lambda_2}(\vec{p})|C_1\bar{C}_2; i\vec{p}\lambda_1\lambda_2JM\rangle\,, \tag{E7}$$

where P_C is the projection operator into the decay sector, $|\alpha JM\rangle$ is an eigenstate of the full Hamiltonian at rest, and $\vec{p}$ is the relative momentum between the two charmed mesons C_1 and $\bar{C}_2$. The coefficient $b^{\alpha J}_{i\lambda_1\lambda_2}(\vec{p})$ is given by (3.51). To compute $\vec{j}^{\,C}_{\alpha\alpha'}$ we need the basic matrix element of the current between charmed mesons,

$$\langle C_\alpha(\vec{p}\lambda)|\vec{j}|C_\beta(\vec{p}'\lambda')\rangle = \delta_{\alpha\beta}\delta_{\lambda\lambda'}\frac{e_\alpha}{(2\pi)^3}\frac{\vec{p}}{m_\alpha}, \tag{E8}$$

where e_α and m_α are the charge and mass of the charmed meson α. In the dipole approximation we find

$$\begin{aligned}\vec{j}^{\,C}_{\alpha\alpha'} &= \langle JM_\alpha|P_C\vec{j}P_C|J'M'\alpha'\rangle \\ &= \frac{1}{(2\pi)^3}\sum_i\sum_{\lambda_1\lambda_2} e_i\int d^3p\, b^{\alpha J*}_{i\lambda_1\lambda_2}(\vec{p})\frac{\vec{p}}{\mu_i}b^{\alpha' J'}_{i\lambda_1\lambda_2}(\vec{p}),\end{aligned} \tag{E9}$$

where μ_i is the reduced mass of the two charmed mesons and e_i the charge of the charmed meson (D, D^*, F or F^*). With the aid of the equation of motion

$$\frac{\vec{p}}{\mu_i} = \frac{1}{i}[\vec{x}, H], \tag{E10}$$

we obtain

$$\vec{j}^{\,C}_{\alpha\alpha'} = \frac{k}{(2\pi)^3}\sum_i\sum_{\lambda_1\lambda_2} e_i\int d^3p\, b^{\alpha J*}_{i\lambda_1\lambda_2}(\vec{p})\vec{\nabla}_p b^{\alpha' J'}_{i\lambda_1\lambda_2}(\vec{p}), \tag{E11}$$

where we have used

$$\vec{x} = -\frac{1}{i}\vec{\nabla}_p. \tag{E12}$$

Equation (E11) is the momentum-space analog of (E2).

To proceed further, we must find an explicit expression for the coefficient $b^{\alpha J}_{i\lambda_1\lambda_2}(\vec{p})$. This is obtained from Eqs. (3.32), (3.50), (3.51), and (D14):

$$b^{\alpha J}_{i\lambda_1\lambda_2}(\vec{p}) = \frac{1}{[3(2\pi)^3]^{1/2}}\sum_{nL}\sum_{lm} B_{LJM}(sJ_1\lambda_1J_2\lambda_2, lm)(-i)^{l+1}I^l_{nL}(\vec{p})Y_{lm}(\hat{p})\frac{a^{\alpha J}_{nL}}{E_{\alpha J}-E_1(p)-E_2(p)}. \tag{E13}$$

The gradient operator in Eq. (E11) can be eliminated using

$$\vec{\nabla}_p[f(p)Y_{lm}(\hat{p})] = -\left(\frac{l+1}{2l+1}\right)^{1/2}\left[f'(p)-\frac{l}{p}f(p)\right]\vec{T}_{l,l+1,m}(\hat{p}) + \left(\frac{l}{2l+1}\right)^{1/2}\left[f'(p)+\frac{l+1}{p}f(p)\right]\vec{T}_{l,l-1,m}(\hat{p}), \tag{E14}$$

where $\vec{T}_{ljm}(\hat{p})$ are the vector spherical harmonics defined by

$$\vec{T}_{ljm}(p) = \sum_{m'\mu}\langle l1m'\mu|jm\rangle Y_{lm'}(\hat{p})\vec{\xi}_\mu. \tag{E15}$$

The $\hat{p}$-angular integration is now elementary. The result can be expressed in terms of the integrals

$$\begin{aligned}K^{\alpha J,\alpha' J',i}_{nLi,n'L',i'}(1) &= \int_0^\infty dp\, p^2\Phi^{l,\alpha Ji}_{nL}(p)^*\left[\frac{d}{dp}\Phi^{l',\alpha' J'i}_{n'L'}(p)-\frac{l'}{p}\Phi^{l',\alpha' J'i}_{n'L'}(p)\right], \\ K^{\alpha J,\alpha' J',i}_{nLi,n'L',i'}(2) &= \int_0^\infty dp\, p^2\Phi^{l,\alpha Ji}_{nL}(p)^*\left[\frac{d}{dp}\Phi^{l',\alpha' J'i}_{n'L'}(p)+\frac{l'+1}{p}\Phi^{l',\alpha' J'i}_{n'L'}(p)\right],\end{aligned} \tag{E16}$$

where

$$\Phi^{l,\alpha Ji}_{nL}(p) = \frac{I^l_{nL}(p)}{E_{\alpha J}-E_1(p)-E_2(p)}. \tag{E17}$$

After the summation over the magnetic quantum numbers is carried out, the final result involves 6-j and 9-j symbols:

$$\begin{aligned}\vec{j}^{\,C}_{\alpha\alpha'} = -\frac{ik}{(2\pi)^3}\left(\frac{2}{3\pi^2}\right)\frac{1}{m_q{}^2a^4\beta^3}(-1)^{M'}\sum_m\vec{\xi}_m\begin{pmatrix}J' & J & 1\\ -M' & M & m\end{pmatrix}\sum a^{\alpha J*}_{nL}a^{\alpha' J'}_{n'L'}[e_iD^{(1)}(JnLl, J'n'L'l', i)K^{\alpha J,\alpha' J',i}_{nLi,n'L',i'}(1) \\ + e_iD^{(2)}(JnLl, J'n'L'l', i)K^{\alpha J,\alpha' J',i}_{nLi,n'L',i'}(2)].\end{aligned} \tag{E18}$$

We list the coefficients $D^{(1)}$ and $D^{(2)}$ for various intermediate states:

(1) The intermediate state i consists of two spin-0 charmed mesons:

$$D^{(1)}(JnLl, J'n'L'l', i) = (-1)^{J-1}\left[\frac{(2L+1)(2L'+1)}{2J'+1}\right]^{1/2}\left(\frac{J'+1}{2J'+3}\right)^{1/2} \times \langle L'100|J'0\rangle\langle L100|J0\rangle\,\delta_{J,J'+1}\delta_{l,J}\delta_{l',J'}, \tag{E19}$$

$$D^{(2)}(JnLl, J'n'L'l', i) = (-1)^{J-1}\left[\frac{(2L+1)(2L'+1)}{2J'+1}\right]^{1/2}\left(\frac{J'}{2J'-1}\right)^{1/2} \times \langle L'100|J'0\rangle\langle L100|J0\rangle\,\delta_{J,J'-1}\delta_{l,J}\delta_{l'J'}. \tag{E20}$$

(2) The intermediate state i consists of a spin-0 and a spin-1 charmed meson:

$$D^{(1)}(JnLl, J'n'L'l', i) = (-1)^{l'}[(2J+1)(2J'+1)(2L+1)(2L'+1)l]^{1/2} \times \langle L'100|l'0\rangle\langle L100|l0\rangle\,\delta_{l,l'+1}\left[\begin{Bmatrix} J' & J & 1 \\ L & L' & 1 \end{Bmatrix}\begin{Bmatrix} 1 & L & L' \\ 1 & l' & l \end{Bmatrix} - \begin{Bmatrix} L & 1 & l \\ 1 & L' & l' \\ J & J' & 1 \end{Bmatrix}\right]. \tag{E21}$$

$$D^{(2)}(JnLl, J'n'L'l', i) = (-1)^{l'}[(2J+1)(2J'+1)(2L+1)(2L'+1)l']^{1/2} \times \langle L'100|l'0\rangle\langle L100|l0\rangle\,\delta_{l,l'-1}\left[\begin{Bmatrix} J' & J & 1 \\ L & L' & 1 \end{Bmatrix}\begin{Bmatrix} 1 & L & L' \\ 1 & l' & l \end{Bmatrix} - \begin{Bmatrix} L & 1 & l \\ 1 & L' & l' \\ J & J' & 1 \end{Bmatrix}\right]. \tag{E22}$$

(3). The intermediate state i consists of two spin-1 charmed mesons:

$$D^{(1)}(JnLl, J'n'L'l', i) = (-1)^{J}\left[\frac{(2L+1)(2L'+1)}{2J'+1}\right]^{1/2}\left(\frac{J'+1}{2J'+3}\right)^{1/2}\langle L'100|J'0\rangle\langle L100|J0\rangle\,\delta_{J,J'+1}\delta_{l,J}\delta_{l',J'}$$
$$+(-1)^{l'}2[(2J+1)(2J'+1)(2L+1)(2L'+1)l]^{1/2} \times \langle L'100|l'0\rangle\langle L100|l0\rangle\,\delta_{l,l'+1}\left[\begin{Bmatrix} J' & J & 1 \\ L & L' & 1 \end{Bmatrix}\begin{Bmatrix} 1 & L & L' \\ 1 & l' & l \end{Bmatrix} + \begin{Bmatrix} L & 1 & l \\ 1 & L' & l' \\ J & J' & 1 \end{Bmatrix}\right], \tag{E23}$$

$$D^{(2)}(JnLl, J'n'L'l', i) = (-1)^{J}\left[\frac{(2L+1)(2L'+1)}{2J'+1}\right]^{1/2}\left(\frac{J'}{2J'+3}\right)^{1/2}\langle L'100|J'0\rangle\langle L100|J0\rangle\,\delta_{J,J'-1}\delta_{l,J}\delta_{l'J'}$$
$$+(-1)^{l'}2\sqrt{(2J+1)(2J'+1)(2L+1)(2L'+1)l'} \times \langle L'100|l'0\rangle\langle L100|l0\rangle\delta_{l,l'-1}\left[\begin{Bmatrix} J' & J & 1 \\ L & L' & 1 \end{Bmatrix}\begin{Bmatrix} 1 & L & L' \\ 1 & l' & l \end{Bmatrix} + \begin{Bmatrix} L & 1 & l \\ 1 & L' & l' \\ J & J' & 1 \end{Bmatrix}\right]. \tag{E24}$$

APPENDIX F. CROSS TERM $\vec{j}^{\,X}_{\alpha\alpha'}$

The cross-term contribution to the $E1$ matrix element defined by

$$\vec{j}^{\,X}_{\alpha\alpha'} = \langle \alpha JM|P_\psi \vec{j} P_C|\alpha' J'M'\rangle + \langle \alpha JM|P_C \vec{j} P_\psi|\alpha' J'M'\rangle, \tag{F1}$$

is not gauge invariant. This raises a tricky problem whose satisfactory solution cannot be found within the patchwork approach of this article. To see this let us expand the state vectors in (F1) as in (3.49), or equivalently,

$$P_\psi|\alpha JM\rangle = \sum_{nL} a^{\alpha J}_{nL}|\psi; nLJM\rangle, \tag{F2}$$

$$P_C|\alpha JM\rangle = \sum_i \sum_{\lambda_1\lambda_2}\int d^3p\, b^{\alpha J}_{i\lambda_1\lambda_2}(\vec{p})|C_1\bar{C}_2; i\vec{p}\lambda_1\lambda_2 JM\rangle, \tag{F3}$$

and consider the matrix element

$$\mathcal{J}_\mu = \langle \psi; nLJM|j_\mu|C_1\bar{C}_2; i\vec{p}\lambda_1\lambda_2 JM\rangle, \tag{F4}$$

$\mathcal{J}_\mu$ can be expressed in terms of the wave functions for the $c\bar{c}$ bound states and charmed mesons. A straightforward calculation gives

$$\vec{\mathcal{J}} = \frac{1}{(2\pi)^{9/2}} \frac{e_q}{\sqrt{3}} \sum_{\{s\}} \int d^3x\, d^3y\, e^{i\mu_c \vec{p}\cdot\vec{y}} \psi^*_{nLJM}(\vec{y} s_1 s_2) \times \phi_1(\vec{x}, s_1 s_1') \phi_2(\vec{x} - \vec{y}, s_2 s_2') \times \chi^\dagger_{-s_1'} \vec{\sigma} \chi_{s_2'} , \tag{F5}$$

$$\mathcal{J}_0 = \frac{1}{(2\pi)^{9/2}} \frac{e_q}{\sqrt{3}} \sum_{\{s\}} \int d^3x\, d^3y\, e^{i\mu_c \vec{p}\cdot\vec{y}} \psi^*_{nLJM}(\vec{y} s_1 s_2) \times \phi_1(\vec{x}, s_1 s_1') \phi_2(\vec{x} - \vec{y}, s_2 s_2') \times \chi^\dagger_{-s_1'} \frac{\vec{\sigma}\cdot\vec{k}}{2m_q} \chi_{s_2'} . \tag{F6}$$

Gauge invariance requires that

$$k^\mu \mathcal{J}_\mu = 0 \tag{F7}$$

and

$$\vec{\mathcal{J}} \to 0, \quad \text{as } k^\mu \to 0 . \tag{F8}$$

As is readily seen, however, (F5) and (F6) satisfy neither of these relations. (But note that $\mathcal{J}_0 \to 0$ for $k^\mu \to 0$.)

How should we understand this failure of gauge invariance? In a covariant Feynman-diagram approach, the contributions $\vec{j}^{\,\psi}_{\alpha\alpha'}$, $\vec{j}^{\,c}_{\alpha\alpha'}$, and $\vec{j}^{\,x}_{\alpha\alpha'}$ must be computed as a whole to ensure gauge invariance. In our noncovariant formulation the contributions $\vec{j}^{\,\psi}_{\alpha\alpha'}$ and $\vec{j}^{\,c}_{\alpha\alpha'}$ are separately gauge invariant which follows from the equation of motion

$$\frac{\vec{p}}{m} = i[H, \vec{x}] \tag{F9}$$

in the respective channel. However, the justification of this equation requires the assumptions that the charmed mesons are pointlike and that the potential is momentum independent. Presumably the failure of $\mathcal{J}_\mu$ to satisfy gauge invariance by itself is a manifestation that these assumptions are not justified and $\vec{j}^{\,\psi}_{\alpha\alpha'}$, $\vec{j}^{\,c}_{\alpha\alpha'}$ are only superficially gauge invariant.

Before we proceed, we must find a gauge-invariant form of $\mathcal{J}_\mu$ which somehow takes care of these problems. To do this correctly would require a complete revamping of our nonrelativistic and phenomenological approach, so we shall adopt here a plausible but totally *ad hoc* assumption that the "charge density" $\mathcal{J}_0$ is correctly given by (F6) but the "current density" $\vec{\mathcal{J}}$ of (F5) must be modified. As is readily seen, gauge invariance can then be restored if we multiply the expression (F5) by $k/2m_q$. We shall choose this as the definition of $\vec{\mathcal{J}}$.

The cross term $\vec{j}^{\,x}_{\alpha\alpha'}$ thus redefined turns out to be reasonably small for the range of parameters we are interested in. Note also that it gives vanishing contribution to the $E1$ moment in the SU(3) symmetric limit.

Substituting Eq. (E3) for ψ_{nLJM} in (F5) and restricting ourselves to S-state charmed mesons, we find

$$\vec{\mathcal{J}} = \frac{k}{(2\pi)^{9/2}\sqrt{3}} \frac{e_q}{2m_q} \sum_{m\lambda} \frac{1}{2\sqrt{2}} \mathrm{Tr}(\Gamma^\dagger_{s\lambda} \Gamma_{s_1\lambda_1} \vec{\sigma} \Gamma_{s_2\lambda_2}) \langle LSm\lambda | JM \rangle \times \int d^3x\, d^3y\, Y^*_{Lm}(\hat{y}) \phi_1(|\vec{x}|) \phi_2(|\vec{x} - \vec{y}|) R_{nL}(|\vec{y}|) e^{i\mu_c \vec{p}\cdot\vec{y}} , \tag{F10}$$

where s_1 and s_2 are the spins of the two charmed mesons and s is the spin of the $c\bar{c}$ system forming the ψ state.

The x integration can be carried out as before using the Gaussian approximation for ϕ_1 and ϕ_2:

$$\int d^3x\, \phi_1(|\vec{x}|) \phi_2(|\vec{x} - \vec{y}|) \propto e^{-\beta y^2/2} . \tag{F11}$$

After the angular integration in $\vec{y}$ we obtain

$$\vec{\mathcal{J}} = \frac{k}{\sqrt{3}(2\pi)^{9/2}} \frac{e_q}{2m_q} \left(\frac{1}{\beta}\right)^{3/2} 4\pi i^L \sum_{m\lambda} \frac{1}{2\sqrt{2}} \mathrm{Tr}[\Gamma^\dagger_{s\lambda} \Gamma_{s_1\lambda_1} \vec{\sigma} \Gamma_{s_2\lambda_2}] \langle LSm\lambda | JM \rangle J_{nL}(p) Y^*_{Lm}(\hat{p}) \tag{F12}$$

where

$$J_{nL}(p) = \int_0^\infty dt\, t^2 e^{-t^2/2} j_L\left(\frac{\mu_c p}{\sqrt{\beta}} t\right) R_{nL}\left(\frac{t}{\sqrt{\beta}}\right) . \tag{F13}$$

Again, we shall restrict ourselves to the radiative transitions among spin-triplet states, i.e., $s = 1$. The spins s_1 and s_2 are also the total angular momenta J_1 and J_2 of the two charmed mesons. If we substitute Eq. (E13) for $b^{\alpha J}_{\lambda_1\lambda_2}$ and the above equation for $\vec{\mathcal{J}}$ we find

$$\langle \alpha JM|P_\psi \vec{j} P_C|\alpha' J'M'\rangle = \frac{-ik}{3(2\pi)^5} \sum_{nL,n'L'} \sum_m \sum_{i\lambda_1\lambda_2} \frac{e_q}{m_q\beta^{3/2}} a_{nL}^{\alpha J *} a_{n'L'}^{\alpha' J'} B_{L'J'M'}(SJ_1\lambda_1 J_2\lambda_2 Lm) \frac{1}{2\sqrt{2}}$$

$$\times \mathrm{Tr}[\Gamma_{s\lambda}^\dagger \Gamma_{J_1\lambda_1} \vec{\sigma} \Gamma_{J_2\lambda_2}] \langle LSm\lambda|JM\rangle K^{(3)}_{nL,n'L'\alpha'J'i}, \tag{F14}$$

where

$$K^{(3)}_{nL,n'L'\alpha'J'i} = \int_0^\infty dp\, p^2 J_{nL}(p) \Phi^{L\alpha' J' i}_{n'L'}(p). \tag{F15}$$

The other term $\langle \alpha JM|P_C \vec{j} P_\psi|\alpha' J'M'\rangle$ is obtained from the above by complex conjugation and the interchange of initial and final states.

After we carry out the summations over magnetic quantum numbers we find

$$\vec{j}^{\,X}_{\alpha\alpha'} = \frac{-ik}{(2\pi)^3} \frac{2}{3(2\pi)^{3/2}} (-1)^{M'} \sum_\mu \vec{\xi}_\mu \begin{pmatrix} J' & J & 1 \\ -M' & M & \mu \end{pmatrix}$$

$$\times \sum_{nLn'L'} \sum_i a_{nL}^{\alpha J *} a_{n'L'}^{\alpha' J'} \frac{e_q}{m_q^2 a^2 \beta^3} [X^{J_1J_2}_{JL,J'L'} K^{(3)}_{nL,n'L'\alpha'J'i} + \bar{X}^{J_1J_2}_{JL,J'L'} K^{(3)}_{n'L',nL\alpha Ji}]. \tag{F16}$$

The coefficients X and $\bar{X}$ are listed below for various intermediate states.

(1) The intermediate state i consists of two spin-0 charmed mesons ($J_1 = J_2 = 0$):

$$X^{J_1J_2}_{JL,J'L'} = \delta_{LJ'}(-1)^{J'-1} \left[\frac{(2J+1)(2L'+1)}{2J'+1}\right]^{1/2} \langle L'100|J'0\rangle, \tag{F17}$$

$$\bar{X}^{J_1J_2}_{JL,J'L'} = \delta_{L'J}(-1)^{J-1} \left[\frac{(2J'+1)(2L+1)}{2J+1}\right]^{1/2} \langle L100|J0\rangle. \tag{F18}$$

(2) The intermediate state i consists of a spin-0 and a spin-1 charmed meson ($J_1 = 0$, $J_2 = 1$ or vice versa):

$$X^{J_1J_2}_{JL,J'L'} = [(2J+1)(2J'+1)(2L'+1)]^{1/2} \langle L'100|L0\rangle \left[(-1)^{L'} \begin{Bmatrix} J & J' & 1 \\ L' & L & 1 \end{Bmatrix} + \frac{1}{2J+1}(-1)^L \delta_{JL'}\right], \tag{F19}$$

$$\bar{X}^{J_1J_2}_{JL,J'L'} = [(2J+1)(2J'+1)(2L+1)]^{1/2} \langle L100|L'0\rangle \left[(-1)^{L} \begin{Bmatrix} J' & J & 1 \\ L & L' & 1 \end{Bmatrix} + \frac{1}{2J'+1}(-1)^{L'} \delta_{J'L}\right]. \tag{F20}$$

(3) The intermediate state i consists of two spin-1 charmed mesons ($J_1 = J_2 = 1$):

$$X^{J_1J_2}_{JL,J'L'} = \delta_{LJ'}(-1)^{J'} \left[\frac{(2J+1)(2L'+1)}{2J'+1}\right]^{1/2} \langle L'100|J'0\rangle$$

$$+ 2[(2J+1)(2J'+1)(2L'+1)]^{1/2} \langle L'100|L0\rangle \left[(-1)^{L'} \begin{Bmatrix} J & J' & 1 \\ L' & L & 1 \end{Bmatrix} - \frac{1}{2J+1}(-1)^L \delta_{JL'}\right], \tag{F21}$$

$$\bar{X}^{J_1J_2}_{JL,J'L'} = \delta_{L'J}(-1)^{J} \left[\frac{(2J'+1)(2L+1)}{2J+1}\right]^{1/2} \langle L100|J0\rangle$$

$$+ 2[(2J+1)(2J'+1)(2L+1)]^{1/2} \langle L100|L'0\rangle \left[(-1)^{L} \begin{Bmatrix} J' & J & 1 \\ L & L' & 1 \end{Bmatrix} - \frac{1}{2J'+1}(-1)^{L'} \delta_{J'L}\right]. \tag{F22}$$

*Present address: Harvard University, Cambridge, MA 02138.
†Address until September 1978: CERN, Geneva, Switzerland.

[1]J. J. Aubert *et al.*, Phys. Rev. Lett. 33, 1404 (1974); J.-E. Augustin *et al.*, *ibid.* 33, 1406 (1974).
[2]G. S. Abrams *et al.*, Phys. Rev. Lett. 33, 1453 (1974).
[3]For a comprehensive review of the data, see G. J. Feldman and M. L. Perl, Phys. Rep. 33C, 285 (1977). When experimental references are not cited explicitly in this article, the data comes from this review.
[4]T. Appelquist and H. D. Politzer, Phys. Rev. Lett. 34, 43 (1975); Phys. Rev. D 12, 1404 (1975).
[5]T. Appelquist, A. De Rújula, H. D. Politzer, and S. L. Glashow, Phys. Rev. Lett. 34, 365 (1975).
[6]E. Eichten, K. Gottfried, T. Kinoshita, J. Kogut, K. D. Lane, and T.-M. Yan, Phys. Rev. Lett. 34, 369 (1975).
[7]A. De Rújula and S. L. Glashow, Phys. Rev. Lett. 34, 46 (1975); C. G. Callan, R. L. Kingsley, S. B. Treiman, F. Wilczek, and A. Zee, *ibid.* 34, 52 (1975); B. J. Harrington, S. Y. Park, and A. Yildiz, *ibid.* 34, 168, 706 (1975); J. S. Kang and H. J. Schnitzer, Phys. Rev. D 12, 841 (1975); 12, 2791 (1975).
[8]G. Goldhaber *et al.*, Phys. Rev. Lett. 37, 255 (1976).
[9]E. Lohrmann in *Proceedings of the 1977 International Symposium on Lepton and Photon Interactions at High Energies, Hamburg*, edited by F. Gutbrod (DESY, Hamburg, 1978).
[10]E. Eichten, K. Gottfried, T. Kinoshita, K. D. Lane, and T.-M. Yan, Phys. Rev. Lett. 36, 500 (1976).
[11]E. Eichten, in *Weak and Electromagnetic Interactions at High Energies*, Proceedings of the Summer Institute, Cargèse, 1975, edited by M. Lévy, J.-L. Basdevant, D. Speiser, and R. Gastmans (Plenum, New York, 1976), part A.
[12]K. Gottfried, in *Proceedings of the Institute of Particle Physics International School on Physics at High Energy Accelerators*, McGill Univ., 1975, edited by R. Henzi and B. Margolis (McGill Univ. Montreal, 1975).
[13]K. Lane and E. Eichten, Phys. Rev. Lett. 37, 477 (1976).
[14]E. Eichten and K. Gottfried, Phys. Lett. 66B, 286 (1977).
[15]S. Weinberg, Phys. Rev. Lett. 31, 494 (1973); D. J. Gross and F. Wilczek, Phys. Rev. D 8, 3633 (1973).
[16]See, however, C. G. Callan, R. Dashen, and D. J. Gross, Inst. for Adv. Study Report No. C00-2220-115, 1977 (unpublished); F. L. Feinberg, Phys. Rev. Lett. 39, 316 (1977); T. Appelquist, M. Dine, and I. Muzinich, Phys. Lett. 69B, 231 (1977); W. Fischler, Nucl. Phys. B129, 157 (1977); E. C. Poggio, Phys. Lett. 71B, 381 (1977). See also the earlier work of A. Duncan, Phys. Rev. D 13, 2866 (1976).
[17]J. Kogut and L. Susskind, Phys. Rev. D 9, 3501 (1974); K. Wilson, *ibid.* D 10, 2445 (1974). See also E. P. Tryon, Phys. Rev. Lett. 28, 1605 (1972).
[18]S. W. Herb *et al.*, Phys. Rev. Lett. 39, 252 (1977).
[19]W. R. Innes *et al.*, Phys. Rev. Lett. 39, 1240, 1640 (E) (1977).
[20]C. Quigg and J. L. Rosner, Phys. Lett. 71B, 153 (1977).
[21]K. Gottfried, in *Proceedings of the 1977 International Symposium on Lepton and Photon Interaction at High Energies*, Hamburg (Ref. 9).
[22]W. Celmaster, H. Georgi, and M. Machacek, Phys. Rev. D 17, 879 (1978); 17, 886 (1978); D. Pignon and C. A. Piketty, Ecole Normale Supérieure, Paris, report, 1977 (unpublished).
[23]See also R. Carlitz and M. Kislinger, Phys. Rev. D 2, 336 (1970); A. LeYaouanc, L. Oliver, O. Pène, and J.-C. Raynal, Phys. Rev. D 8, 2223 (1973).
[24]Note that this differs somewhat from the viewpoint we had adopted in Refs. 6 and 14.
[25]J. Pumplin, W. Repko, and A. Sato, Phys. Rev. Lett. 35, 1538 (1975) H. J. Schnitzer, *ibid.* 35, 1540 (1975); Phys. Rev. D13, 74 (1976); A. B. Henriques, B. H. Kellett, and R. G. Moorhouse, Phys. Lett. 64B, 85 (1976).
[26]J. Schwinger, Harvard lectures (unpublished).
[27]G. Goldhaber *et al.*, Phys. Lett. 69B, 503 (1977).
[28]The proposal that nodes in the decay amplitude of the radially excited 3S level are responsible for the remarkable ratios of charmed meson production was put forward independently by A. Le Yaouanc, L. Oliver, O. Pène, and J. C. Raynal, Phys. Lett. 71B, 397 (1977); *ibid.* 72B, 53 (1977).
[29]P. A. Rapidis *et al.*, Phys. Rev. Lett. 39, 526 (1977).
[30]This model therefore differs from that of Carlitz and Kislinger, and of LaYaouanc *et al.* (Ref. 23), where the pair is created in the scalar $^3P_0$ state. ^1S-pair creation is a consequence of our assumption of one-gluon exchange, which has the merit of simplicity, but is not well founded theoretically. In particular, it has recently been shown [K. Gottfried, Phys. Rev. Lett. 40, 598 (1978)] that certain intrinsically non-Abelian graphs dominate in the limit of large m_Q. Whether this limit is relevant to charmonium is not known.
[31]H. Feshbach, Ann. Phys. (N.Y.) 5, 357 (1958). For other applications, see K. Gottfried, in *1967 Brandeis University Summer Institute in Theoretical Physics*, edited by M. Chrétien and S. S. Schweber (Gordon and Breach, New York, 1970), Vol. 2.
[32]The mathematical foundation of the formalism adopted here has been thoroughly investigated by R. F. Dashen, J. B. Healy, and I. J. Muzinich, Phys. Rev. D14, 2773 (1976).
[33]V. N. Gribov, Zh. Eksp. Teor. Fiz. 57, 1306 (1969) [Sov. Phys.—JETP 30, 709 (1970)]; S. J. Brodsky and J. Pumplin, Phys. Rev. 182, 1794 (1969).
[34]We thank R. N. Cahn for bringing a numer of errors in this appendix to our attention.